

**Investigating use of metal-modified HZSM-5 catalyst to  
upgrade liquid yield in co-pyrolysis of Wheat Straw and  
Polystyrene**



Author

Madiha Razzaq

Regn Number

00000172782

Supervisor

Dr. Muhammad Zeeshan Ali Khan

INSTITUTE OF ENVIRONMENTAL SCIENCES AND ENGINEERING (IESE)  
SCHOOL OF MECHANICAL & MANUFACTURING ENGINEERING  
NATIONAL UNIVERSITY OF SCIENCES AND TECHNOLOGY  
ISLAMABAD  
2016-2018

Investigating use of metal-modified HZSM-5 catalyst to upgrade liquid  
yield in co-pyrolysis of Wheat Straw and Polystyrene

Author

Madiha Razzaq

Regn Number

00000172782

A thesis submitted in partial fulfillment of the requirements for the degree of  
MS Environmental Engineering

Thesis Supervisor:

Dr. Muhammad Zeeshan Ali Khan

Thesis Supervisor's Signature: \_\_\_\_\_

INSTITUTE OF ENVIRONMENTAL SCIENCES AND ENGINEERING (IESE)  
SCHOOL OF MECHANICAL & MANUFACTURING ENGINEERING  
NATIONAL UNIVERSITY OF SCIENCES AND TECHNOLOGY,  
ISLAMABAD  
2016-2018

## **Declaration**

I certify that this research work titled “*Investigating use of metal-modified HZSM-5 catalyst to upgrade liquid yield in co-pyrolysis of Wheat Straw and Polystyrene*” is my own work. The work has not been presented elsewhere for assessment. The material that has been used from other sources it has been properly acknowledged / referred.

---

Madiha Razzaq

## **Plagiarism Certificate (Turnitin Report)**

This thesis has been checked for Plagiarism. Turnitin report endorsed by Supervisor is attached.

Signature of Student

Madiha Razzaq

00000172782

Signature of Supervisor

## **Copyright Statement**

- Copyright in text of this thesis rests with the student author. Copies (by any process) either in full, or of extracts, may be made only in accordance with instructions given by the author and lodged in the Library of Institute of Environmental Sciences and Engineering (IESE). Details may be obtained by the Librarian. This page must form part of any such copies made. Further copies (by any process) may not be made without the permission (in writing) of the author.
- The ownership of any intellectual property rights which may be described in this thesis is vested in of Institute of Environmental Sciences and Engineering (IESE), subject to any prior agreement to the contrary, and may not be made available for use by third parties without the written permission of the IESE, which will prescribe the terms and conditions of any such agreement.
- Further information on the conditions under which disclosures and exploitation may take place is available from the Library of Institute of Environmental Sciences and Engineering (IESE), Islamabad.

## **Acknowledgements**

I am thankful to my Creator Allah Subhana-Watala to have guided me throughout this work at every step and for every new thought which You setup in my mind to improve it. Indeed, I could have done nothing without Your priceless help and guidance. Whosoever helped me throughout the course of my thesis, whether my parents or any other individual was Your will, so indeed none be worthy of praise but You.

I am profusely thankful to my beloved parents who raised me when I was not capable of walking, continued to support me throughout in every department of my life and remained patient when I claimed my thesis would be finished 'in the next month' for nearly a half year.

I owe my deepest gratitude to my supervisor Dr. Zeeshan Ali Khan. His guidance, patience and help in dealing with the many challenges of this research, have been invaluable. I am also greatly indebted for Air and Noise Pollution Control and Modeling of Environmental Systems subjects which he has taught me. I can safely say that I haven't learned any other engineering subject in such depth than the ones which he has taught.

I would also like to pay special thanks to Sir Saeed for his tremendous support and cooperation. Each time I got stuck in something, he came up with the solution. I appreciate his patience and guidance throughout the whole thesis.

I would also like to thank Dr. Sara Qaiser and Dr. Yousuf Jamal for being on my thesis guidance and evaluation committee and express my special thanks to Sir Basharat for his continuous help.

My acknowledgement will never be complete without the special mention of my friends: Bushra Muneer & Hera Iftikhar, who have always been there and bearing with me the good and bad times during my wonderful days of thesis. I can't imagine any better collaboration than what I had with them. I would also like to acknowledge my friend Mariam Sabeeh for her moral support and motivation, which drives me to give my best.

Finally, I would like to express my gratitude to all the individuals who have rendered valuable assistance to my study.

*Dedicated to my exceptional parents and adored siblings whose  
tremendous support and cooperation led me to this wonderful  
accomplishment.*

## Abstract

Co-pyrolysis of wheat straw (WS) and polystyrene (PS) at a weight ratio of 1:1 was conducted in a fixed bed reactor. The effect of ex-situ application of HZSM-5 and its metal modified versions (MZSM-5s) on organic liquid product (OP) upgradation was explored. MZSM-5s were synthesized by adding metal (Co, Ni, Zn and Fe) oxides to parent HZSM-5 catalyst through wet impregnation method. The catalysts were characterized by XRD, SEM-EDS, and N<sub>2</sub> physisorption. In first phase, the effect of co-pyrolysis temperature (500-650 °C) on product distribution was evaluated. The liquid yield varied in the range of 49–55 wt.%, with a maximum at 550 °C. In second phase, results obtained from vapor catalyzed co-pyrolysis conducted at 550 °C showed that impregnation of HZSM-5 with metals resulted in relatively higher OP oil yield as compared to parent HZSM-5. Co-ZSM-5 produced maximum OP yield (39.0%) followed by Zn-ZSM-5 (38.2%), Fe-ZSM-5 (37.7%) and Ni-ZSM-5 (36.1%). Whilst, the coke yield was reduced for all MZSM-5s by approximately 50%. Moreover, the addition of metals significantly favored the catalytic selectivity towards monoaromatic hydrocarbons (MAHs). Fe-ZSM-5 proved to be most effective catalyst exhibiting the highest de-oxygenation potential (97.4%) and displaying maximum MAHs content (83.3%). Simultaneously, MZSM-5s reduced undesirable polyaromatic hydrocarbons (PAHs) yield noticeably.



**Key Words:**

BET	Brunauer–Emmett–Teller
BTX	Benzene, Toluene, Xylene
CFP	Catalytic Fast Pyrolysis
C/F	Catalyst to Feedstock ratio
EDS	Energy dispersive spectroscopy
GC-MS	Gas Chromatograph Mass Spectrometer
HHV	High heating value
ZSM-5	Zeolite Socony Mobil -5
MAH	Mono aromatic hydrocarbons
NIST	National Institute of Standards and Technology
Py-GC/MS	Pyrolysis-gas chromatography/mass spectrometry
PAH	Polyaromatic hydrocarbons
PS	Polystyrene
PP	Polypropylene
HDPE	High Density Polyethylene
LDPE	Low Density Polyethylene
SAR	Silica to Alumina ratio
SEM	Scanning electron microscopy
TGA	Thermogravimetric analysis
TMR	Tandem Micro-Pyrolyser
WS	Wheat Straw
WGS	Water Gas Shift
XRD	X-ray diffraction

# Table of Contents

<b>Declaration</b> .....	<b>i</b>
<b>Plagiarism Certificate (Turnitin Report)</b> .....	<b>ii</b>
<b>Copyright Statement</b> .....	<b>iii</b>
<b>Acknowledgements</b> .....	<b>iv</b>
<b>Abstract</b> .....	<b>vi</b>
<b>Table of Contents</b> .....	<b>viii</b>
<b>List of Figures</b> .....	<b>xi</b>
<b>List of Tables</b> .....	<b>xii</b>
<b>Chapter 1 INTRODUCTION</b> .....	<b>1</b>
1.1. Background.....	1
1.2. Problem statement .....	2
1.3. Research objectives .....	3
<b>Chapter 2 LITERATURE REVIEW</b> .....	<b>1</b>
2.1 Energy background.....	1
2.2 Biomass energy application.....	2
2.3 Types of biofuels .....	4
2.4 Structure and composition of biomass.....	5
2.5 Biomass conversion methods .....	5
2.6 Pyrolysis .....	6
2.6.1. Pyrolysis products.....	7
2.6.2. Advantages of bio-oil .....	8
2.6.3. Pyrolysis Mechanism.....	9
2.6.4. Factor affecting pyrolysis process .....	10
2.6.4.1. Temperature .....	10

2.6.4.2.	Biomass heating rate .....	11
2.6.4.3.	Biomass type .....	11
2.6.4.4.	Sweep Gas flow rate.....	12
2.6.4.5.	Types of pyrolysis reactors .....	13
2.6.5.	Drawbacks of bio-oil .....	15
2.6.6.	Upgradation of un-processed bio-oil .....	16
2.7.	Upgradation methods.....	17
2.7.1.	Catalytic upgradation.....	17
2.7.1.1.	Cracking mechanism .....	18
2.7.1.2.	Types of catalyst.....	18
2.7.1.3.	Zeolite ZSM-5 .....	21
2.7.1.4.	Factors affecting pyrolysis over ZSM-5.....	22
2.7.1.5.	Challenges in cracking over ZSM-5.....	25
2.7.1.6.	H/C <sub>eff</sub> ratio .....	25
2.7.1.7.	ZSM-5 modification .....	27
2.7.1.8.	Metal modified ZSM-5.....	27
2.7.2.	Copolyrolysis.....	32
2.7.3.	Catalytic co-pyrolysis.....	32
<b>Chapter 3</b>	<b>MATERIALS AND METHODS.....</b>	<b>36</b>
3.1	Feedstock preparation.....	36
3.2	Catalyst preparation.....	37
3.3	Pyrolysis Setup & Operation .....	38
3.4	Experimental design .....	40
3.5	Oil separation.....	41
3.6	Catalyst characterization.....	41

3.6.1	N <sub>2</sub> physisorption .....	41
3.6.2	Powder X-ray diffraction (XRD) spectroscopy .....	42
3.6.3	SEM-EDS .....	42
3.7	Liquid product analysis .....	42
4.2.1.	3.7.1. GC-MS.....	42
4.2.2.	3.7.2. Physical properties.....	43
<b>Chapter 4 RESULTS AND DISCUSSION .....</b>		<b>44</b>
4.1	Feedstock analysis .....	44
4.1.1.	Physicochemical characteristics of feedstocks.....	44
4.1.2.	Thermal degradation of feedstocks .....	45
4.2	Catalyst Characterization.....	47
4.2.1	XRD results .....	47
4.2.2	SEM analysis .....	48
4.2.3	EDS analysis.....	49
4.2.4	Textural properties of catalyst .....	50
4.3.	Product analysis.....	50
4.3.1.	Effect of temperature on product yield.....	50
4.3.2.	Effect of metal loaded catalysts on product yield.....	51
4.3.3.	Chemical properties of OP .....	53
4.3.4.	Physical properties of OP .....	55
<b>Chapter 5 CONCLUSIONS AND RECOMMENDATIONS .....</b>		<b>57</b>
<b>REFERENCES.....</b>		<b>59</b>

## List of Figures

Figure 2.1: Worldwide biomass distribution as primary resource .....	4
Figure 2.2: Structural composition of biomass .....	5
Figure 2.3: Various chemical compounds found in bio-oil .....	7
Figure 2.4: Various applications of pyrolysis oil.....	8
Figure 2.5: Pathways involved in conversion of biomass during pyrolysis .....	10
Figure 2.6: Mechanisms involved in catalytic cracking .....	18
Figure 2.7: 3D structure of HZSM-5 .....	21
Figure 2.8: Cracking mechanism of bi-functional catalyst.....	28
Figure 3.1: Feedstock preparation (a) Raw form (b) Shredded form (c) Grinded form .....	36
Figure 3.2: Catalyst preparation (a) Parent HZSM-5 (b) Paste formation (c) Extrusion (d) Fe-ZSM-5 (e) Zn-ZSM-5 (f) Co-ZSM-5 .....	38
Figure 3.3: The schematic diagram of experimental setup .....	40
Figure 4.1: TGA plot of WS and PS .....	46
Figure 4.2: XRD patterns of parent and metal based catalysts .....	47
Figure 4.3: SEM images of (a) Parent HZSM-5 (b) Fe-ZSM-5 (c) Co-ZSM-5 (d) Ni-ZSM-5 (e) Zn-ZSM-5 .....	48
Figure 4.4: EDS analysis of (a) Fe-ZSM-5 (b) Ni-ZSM-5 (c) Zn-ZSM-5 (d) Co-ZSM-5 .....	49
Figure 4.5: Products' distribution at varying temperatures .....	51
Figure 4.6: Pyrolytic products obtained with and without catalysts.....	52
Figure 4.7: Chemical distribution of organic liquid product with and without catalyst .....	54

## List of Tables

Table 0.1: Comparison of properties of bio-oil in comparison with diesel and gasoline .....	9
Table 0.2: Modes of Pyrolysis process w.r.t. heating rates.....	11
Table 2.3: Pyrolysis products obtained from different types of feedstocks.....	12
Table 2.4: Use of different catalysts in upgradation .....	20
Table 0.5: Use of HZSM-5 for catalytic upgrading.....	24
Table 0.6: Effective hydrogen to carbon ratio of different biomasses.....	26
Table 2.7: Catalytic upgrading of different biomass over metal modified HZSM-5 catalysts.....	30
Table 0.8: Use of HZSM-5 catalyst in conjunction with different plastics for upgrading .....	34
Table 0.1: Physico-chemical characteristics of selected feedstocks.....	44
Table 0.2: Metal content in modified catalysts.....	49
Table 0.3: Porosity characteristics of parent and metal based catalysts .....	50
Table 0.4: Physical properties of liquid oil.....	56

# Chapter 1 INTRODUCTION

## 1.1 Background

Growing energy requirement, declining fossil fuel reserves and ever-increasing environmental threats have made unequivocally crucial to find sustainable and environment friendly sources of energy (Guda et al., 2016; Zheng et al., 2017). In this regard, recent research work has been shifted to investigate lignocellulosic biomass as a potential candidate to harness energy. Moreover, biomass derived fuels may contribute to alleviate worldwide greenhouse gas emissions (Kabir et al., 2017). In Pakistan, 12-15 million tons of crop residues are produced on annual basis, which has insignificant economic use. Pakistan is focusing on utilizing indigenous renewable energy sources in order to cope with current energy demand. However, Pakistan is still lagging behind the right methodology and execution of biomass as an alternative renewable energy resource (Naqvi et al., 2018).

Pyrolysis, an effective thermochemical process, can convert cheap and local biomass to liquid fuel that can be a precursor to valuable chemicals and motor fuels (E. B. Hassan et al., 2016). Pyrolysis process entails thermochemical degradation of carbonaceous biomass in an inert atmosphere at temperature ranging from 400-650 °C. Bio-oil, a dark brown organic liquid, is considered as a promising energy carrier (Iliopoulou et al., 2012). However, crude bio-oil experiences certain undesirable properties such as low calorific value, high oxygen content (30-40 wt.%) and water content, high viscosity and density, corrosive nature, thermal instability during storage, extreme ignition delay and incomplete volatility (Mihalcik et al., 2011). All these characteristics render the bio-oil incompatible with standard petroleum-based refineries. In order to make bio-oil equivalent to customary petroleum fuel and economically attractive it is inevitable to upgrade bio-oil (Carpenter et al., 2014). The focal objective of the upgrading process is to eliminate reactive oxygenated compounds. In this respect, various mechanisms such as hydrodeoxygenation, catalytic upgrading, esterification, steam reforming, super critical extraction, emulsification etc. have been reported in literature (Uzoejinwa et al., 2018).

Based on literature findings, thermo-catalytic pyrolysis has been realized as a robust method in order to obtain upgraded oil (Iliopoulou et al., 2012). Application of heterogeneous catalyst in pyrolysis process with the purpose to expel the reactive oxygenated compounds seems to be most pragmatic (Mihalcik et al., 2011). A plethora of catalysts have been investigated in an attempt to upgrade bio-oil. Zeolite has received increasing attention due to its low price, massive availability and facile tunability. The extensive research in catalyst screening and design has elucidated the zeolite ZSM-5, a highly effective and promising catalyst in terms of its strong ability of deoxygenation and shape selectivity. ZSM-5 zeolite is characterized by three-dimensional crystalline structure having interconnected network of channels (Zig Zag and linear), intermediate pore size (0.52-0.56 nm), better acidity, higher resistance to deactivation. Micropores of ZSM-5 allow to enter small molecules which are then folded to aromatics (E. B. Hassan et al., 2016; S. Liu et al., 2017)

## **1.2 Problem statement**

A major drawback associated with thermo-catalytic upgrading over ZSM-5 is coke deposition on catalyst which leads to catalyst deactivation. It is discerned that coke formation is primarily associated with low hydrogen content of lignocellulose biomass (Zhang et al., 2016). Therefore, there is need to introduce hydrogen sources either by direct injecting hydrogen gas or by modifying reaction environment. Introduction of molecular hydrogen is not cost-effective method. This can be achieved via modification of acidic ZSM-5 catalyst or incorporation of a hydrogen donor during catalytic reactions. Increasing attention is now being paid to modify ZSM-5/ HZSM-5 by incorporation of metals within catalyst structure. Promotion of ZSM-5 with different metals such as, lead, nickel, Cobalt, Iron, Gallium, Tin, Zinc, Cerium etc. have been reported in literature (S. Zhang et al., 2018). Incorporation of transition metals is suggested to affect the mechanism of oxygen removal in a way that it rejects oxygen more in the form of carbon oxides instead of water, thus provides more hydrogen available for hydrocarbon production (French et al., 2010).



Modified catalyst produce hydrogen through WGS reaction (Kantarelis et al., 2014). It has been confirmed that modification of ZSM-5 with metals alter acid site and textural properties of catalyst (Botas et al., 2012). This is helpful in attenuating rate of coke formation over catalyst and improve liquid product yield. ZSM-5 doped with metals was also considered to improve hydrothermal stability of the catalyst (Iliopoulou et al., 2012). Metal modified ZSM-5 promotes aromatization reactions resulting in enhanced selectivity toward aromatic compounds (Iliopoulou et al., 2014). Incorporation of hydrogen rich feedstock in catalytic pyrolysis of biomass could be helpful in mitigating problems such as high coke deposition over catalyst and low carbon yield. Waste plastics can be exploited as potential hydrogen donor as they are rich in hydrogen. Massive quantities of plastic waste, generated each year present a cheap and abundant co-reactant to be incorporated in catalytic co-pyrolysis (Wang et al., 2013).

### **1.3 Research objectives**

The two main objective of this study are as follows.

- Optimize the reaction temperature for co-pyrolysis of wheat straw and polystyrene
- Compare and evaluate the catalytic performance of HZSM-5& metal assisted HZSM-5 for upgrading liquid yield in co-feed of wheat straw and polystyrene at optimized temperature

## Chapter 2 LITERATURE REVIEW

This chapter presents a comprehensive review on energy background (international & national), application of biomass as energy source and structure of biomass. It further provides insight into pyrolysis process; its products and mechanism, pros and cons of bio-oil. It also discusses progress on catalytic up gradation of bio-oil, challenges in catalytic cracking accompanied by ways to overcome them and catalytic copyrolysis method.

### 2.1 Energy background

Energy is indispensable for the development of world's economy (Asadullah et al., 2007). Global energy demand is growing steadily due to ever-increasing population and tremendous technological development in every aspect of life. The gap between energy supply and demand is widening day by day. Energy consumption of a country is an indicator of prosperity of the people living there (M. Mujahid Rafique et al., 2017). According to US Energy Information Administration, a major fraction (approximately 79%) of world's energy need is still catered by traditional fossil fuels such as coal, natural gas and petroleum (Gollakota et al., 2016).

According to an estimate, worldwide daily consumption of liquid fuel is approximately 97.51 million barrels (Rahman et al., 2018). Transportation fuel demand is one fifth of total energy demand and is currently derived by fossil fuels (Rezaei et al., 2017). Moreover, fossil fuels are sources of various industrial organic chemicals. As a result, these resources are being exploited at a rate faster than their natural deposition creating an imbalance between energy supply and demand (Islam et al., 2017). The exhaustion of these fuels is expected to become double by 2050 compared to present (Bulushev et al., 2011).

Pakistan is facing serious energy crisis, which leads to adverse socio-economic problems. Much of the people especially in northern areas do not have access to modern energy facilities. Pakistan has limited fossil fuel reserves, which oblige the country to spend more than 60% of its foreign exchange on importing fossil fuels (M Mujahid Rafique et al., 2017). This results in high costs of fossil fuels (Naqvi et al., 2018).

At the same time, intensive use of fossil fuels for energy production is creating serious environmental concerns such as global warming, atmospheric pollution, acid rain etc. Greenhouse gases (GHGs), primarily CO<sub>2</sub>, emitted as a result of burning fossil fuels, accounts for two-thirds of anthropogenic CO<sub>2</sub> emissions worldwide. These emissions are responsible for global warming (Mohan et al., 2006). Growing energy requirement, finite oil supplies, declining fossil fuel reserves, increasing oil prices, ever increasing environmental threats and emphasis on greenhouse emissions reduction have made unequivocally crucial to find sustainable and environment friendly sources of energy (Zheng et al., 2017).

The development of numerous renewable energy technologies has led to production of solar, tidal, geothermal, wind, hydroelectric power etc. in order to combat global energy shortfall. All these technologies are destined to reduce reliance on fossil fuel-based energy production without environmental degradation. According to an estimate, European Union (EU) is producing 71% of electrical energy from renewable energy sources (Naqvi et al., 2018). However, current infrastructure necessitates the production of hydrocarbons for synthesis of various goods including plastics, hydraulic fluids, lubricating oil in addition to fuel oil (Dickerson et al., 2013).

## **2.2 Biomass energy application**

Recent research work has been shifted to investigate lignocellulosic biomass as a source of several fuel types (solid, liquid and gaseous) and valuable chemicals (Kabir et al., 2017). Biomass is material derived from plants growth and from animal manure. Humans have used the biomass as an energy source for thousands of years (Mirza et al., 2008). At present, biomass is the fourth largest energy source after conventional fuels

(coal, natural gas, petroleum) and contributes to about 18% of global energy supply (Gollakota et al., 2016; Iliopoulou et al., 2012). It is the only renewable energy source that has potential to provide competitively priced petroleum like products (E. B. Hassan et al., 2016).

As compared to traditional fossil fuels, substantial masses of biomass can be produced annually thus can provide continuous energy supply. It is estimated that almost 220 billion tons of biomass is being produced globally on annual basis (H. Hassan et al., 2016). Abundance and renewable nature of biomass makes it a world's largest sustainable energy resource (S. Liu et al., 2017) The European Union renewable roadmap have set the target that every EU member should meet 10% of its fuel demand by biofuel by 2020 (Bulushev et al., 2011). Biomass derived fuels may contribute to alleviate worldwide greenhouse gas emissions, mainly CO<sub>2</sub>. CO<sub>2</sub> evolved as a result of combustion of biofuels is consumed back during plant photosynthesis, thus making it a carbon neutral process (Kabir et al., 2017).

More than 60% of Pakistan's economy is dependent on agriculture and about 62% of population lives in rural areas (Naqvi et al., 2018). In rural and low-income urban areas, biomass (crop residues, firewood, and animal manure) is being used to cope with everyday energy requirement mainly through combustion. Firewood is commonly used for heating purposes. Based on Household Energy Strategy Study (1992), it was estimated that biomass contribute up to 27% of total energy supply in Pakistan with firewood, the largest contributor (60%) followed by crop residues (21%) and animal waste (19%). It has been reported that, in Pakistan, 12-15 million tons of crop residues are produced on annual basis, which has insignificant economic use. Sugarcane, wheat straw, rice husk and maize are the main agricultural waste materials. These crop residues can contribute to encounter 76% Pakistan's current energy demand. Unfortunately, a major fraction of crop residues is burnt instead of using it as energy source (Mirza et al., 2008).

### 2.3 Types of biofuels

Biomass derived fuels are categorized as primary and secondary biofuels. Primary biofuels are those where biomass is employed in an unprocessed form for energy extraction purposes e.g. cooking, power production, heating etc. Wood can be taken as primary biofuel. Secondary biofuels are derived by processing of biomass. These fuels include bioethanol, biodiesel etc. (Güngör et al., 2012).

Secondary biofuels are produced using three “generations” technologies. At present, biofuels are being produced using “First Generation” technology that allows the use of biomass suitable for food e.g. rapeseed, corn etc. Deployment of “first generation” technology may have adverse impacts on food market and prices. The “Second Generation” technology utilizes non-food lignocellulosic feedstock e.g. agricultural residues, forestry waste, industrial and municipal wastes, grasses and some specially grown crops (miscanthus and sorghum). This technology is beneficial as it does not disturb food chain (Bulushev et al., 2011). It is approximated that 150-170 billion tons non-food lignocellulosic biomass is produced every year (Kabir et al., 2017). The developed countries are incorporating waste biomass as a feedstock in energy production sector. The “third generation” technology generally use genetically modified feedstock e.g. genetically modified algae for biofuels production (Bulushev et al., 2011).

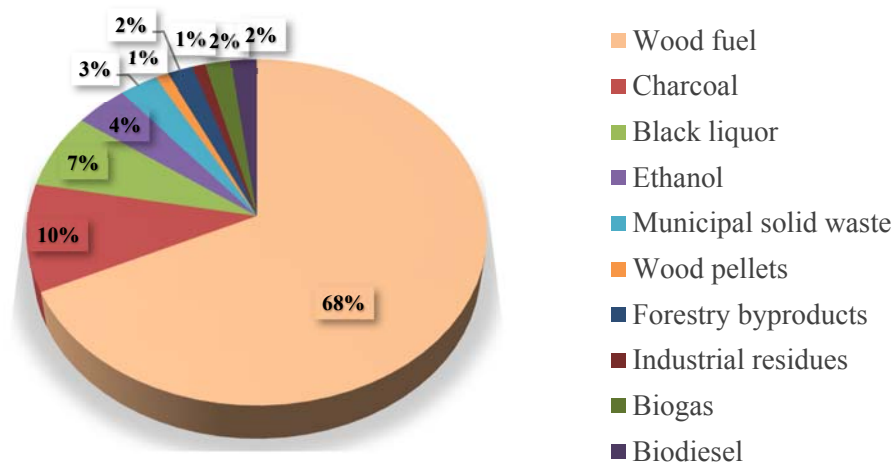


Figure 2.1: Worldwide biomass distribution as primary resource

## 2.4 Structure and composition of biomass

Lignocellulosic biomass is synthesized using atmospheric carbon dioxide, water, solar energy and some essential nutrients through process of photosynthesis. Biomass is primarily constituted by three polymers i.e. lignin, hemicellulose and cellulose. Cellulose and hemicellulose are carbohydrate components whereas lignin is a complex polymer consists of hydroxyl and methoxy substituted phenylpropene units (Collard et al., 2014). Hemicellulose is covered by cellulose and both are enclosed by lignin. Lignin is responsible for providing structural strength to each part of plant. All three components exhibit different behavior during decomposition (Jahirul et al., 2012).

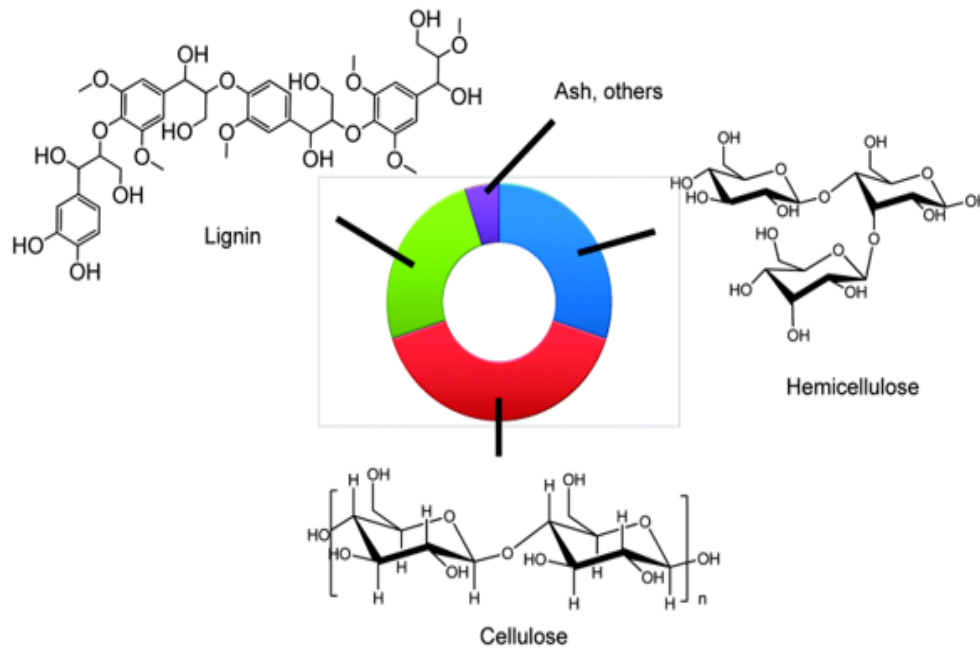


Figure 2.2: Structural composition of biomass

## 2.5 Biomass conversion methods

Various methods have been employed to convert biomass into valuable hydrocarbons.

These methods include

- Physicochemical
- Thermochemical
- Biochemical

Physio-chemical methods involves the use of physical and chemical processes at near atmospheric pressure and ambient temperature. Transesterification is a popular physio-chemical method. Biochemical methods involve synthesis of gaseous and liquid products by using microorganism, enzymes etc. Anaerobic Digestion, hydrolysis and fermentation are examples of bio-chemical method. Bio-chemical methods are not considered cost effective as they only utilize cellulose and hemicellulose for energy production (Zhang et al., 2016). Thermochemical methods employ thermal degradation of biomass to attain desired products. It commonly includes pyrolysis, torrefaction, combustion, gasification and liquefaction (Gollakota et al., 2016).

Thermochemical method is one amongst the aforementioned methods which is gaining significant interest for conversion of biomass to biofuel as they are cost effective and energy efficient. In combustion, fuel is oxidized and converted to heat. This method is only 10% efficient and a source of pollution. Gasification is carried out in a partially oxidizing environment and focuses on production of gaseous fuel e.g. methane. Pyrolysis, an endothermic process, is accomplished in the absence of oxygen (Jahirul et al., 2012).

## **2.6 Pyrolysis**

Pyrolysis, an effective thermochemical process, has gained crucial attention in past few decades as it can convert cheap and local biomass to liquid fuel that can be a precursor to valuable chemicals and motor fuels (Zhang et al., 2016). Pyrolysis embroils thermochemical degradation of carbonaceous biomass in an inert atmosphere i.e. the absence of oxygen, at moderate temperature ranging from 400-650 °C (Dorado et al., 2015). Pyrolysis process is performed in a closed reactor system. Three basic steps involved in the process are sample preparation, pyrolysis and condensation. Biomass sample must be grinded to required size i.e. 2-3mm in order to achieve high heat diffusion through particles. Moisture content is reduced to less than 10%. Oxygen free environment is established mostly by sweeping an inert gas e.g. N<sub>2</sub>, He, Ar etc. (Abnisa et al., 2014)

### 2.6.1. Pyrolysis products

This process yields volatile and non-volatile products, proportion of which can be varied depending upon process variables such as type of pyrolysis system used and mode of pyrolysis (slow or fast). Nonvolatile species are solids and minerals left in reactor, known as biochar. A portion of gas phase volatile species consists of non-condensable gases mainly consisting of CO, CO<sub>2</sub>, CH<sub>4</sub>, H<sub>2</sub> etc. while remaining is condensed to black liquid fuel frequently known as bio-oil or pyrolysis oil (Dickerson et al., 2013).

The pyrolysis process is basically meant for the production of liquid fuel however bio-char and non-condensable gases are collected as by products depending upon process conditions (Carpenter et al., 2014) Bio-oil may contain up to 75% of original feedstock energy content. In pyrolysis, no waste component is produced as bio-char could be used as soil conditioner while gas fraction can be applied as heat source for the process (Güngör et al., 2012).

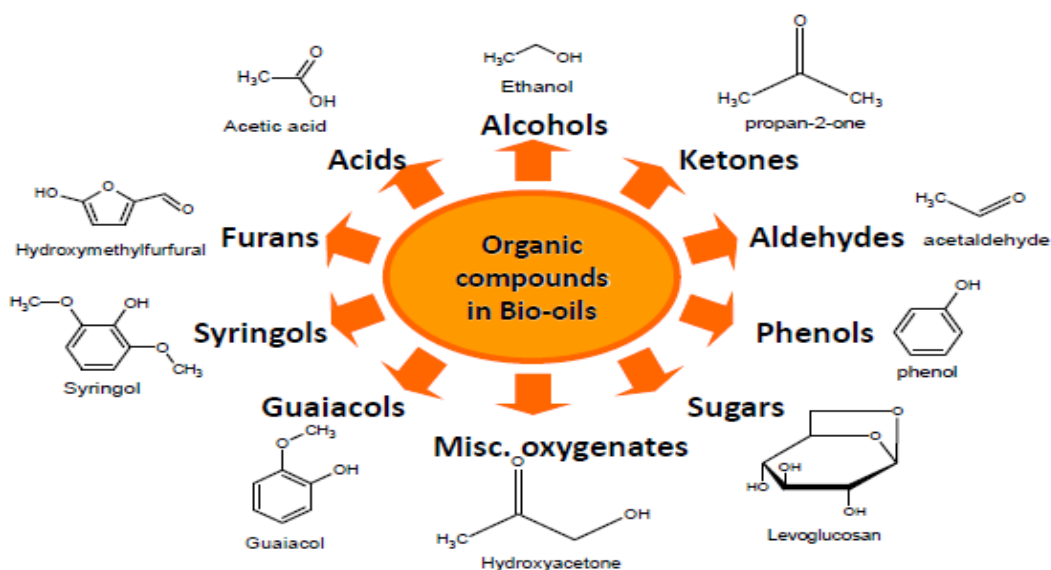


Figure 2.3: Various chemical compounds found in bio-oil

Bio-oil, a dark brown organic liquid, is considered as a promising energy carrier and mainly consists of three types of chemical species i.e. sugar derived, lignin derived and small carbonyl compounds (Iliopoulou et al., 2012). Some common organic compounds



which are generally found in bio-oil are shown in figure above. Fast pyrolysis of biomass may yield up to 70-80% of bio-oil on dry feed basis, under optimized conditions. Temperature higher than 600 °C favors the production of gaseous products while at low heating rates and lower temperature (around 400 °C), bio-char formation is increased. Recent research is aiming to develop conditions of pyrolysis that give optimum yield of bio-oil (Jahirul et al., 2012). Typical applications of bio-oil are depicted in figure 2.4.

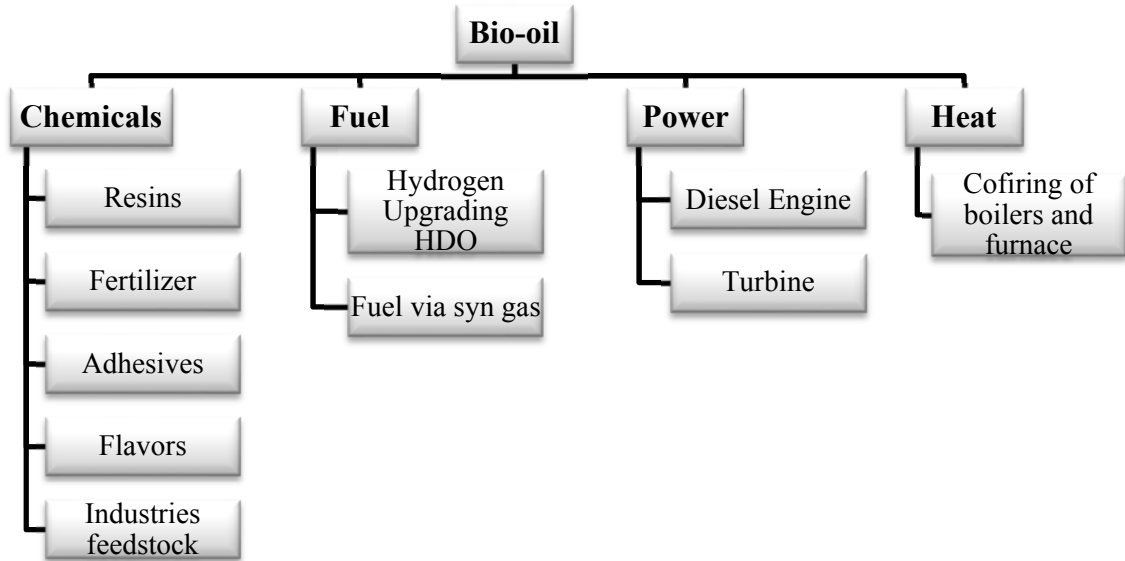


Figure 2.4: Various applications of pyrolysis oil

### 2.6.2. Advantages of bio-oil

Bio-oil is easily transportable fuel and present higher energy content compared to actual biomass (Bulushev et al., 2011). It can be directly utilized in gas turbines and thermal power stations or it can be a precursor to produce different chemicals. It presents potential petrochemical feedstock that can be incorporated into current petroleum-based infrastructure for the production of lighter hydrocarbons such as gasoline or diesel. It is relatively cleaner fuel due to separation of some impurities such as mineral and metals from bio-oil as they are left in biochar (Iliopoulou et al., 2012).

Bio-oil consumption does not produce SO<sub>2</sub> emissions as biomass contains insignificant sulfur content. Furthermore, generated NO<sub>x</sub> emissions are 50% less than diesel fuel (Mohan et al., 2006). This is advantageous from both environmental

standpoint and its post treatment. Some promising properties of bio-oil include good lubricity, less toxicity and greater bio-degradation potential (Gollakota et al., 2016). Comparison of some attributes of bio-oil with petroleum fuels is shown in Table 2.1.

Table 2.1: Comparison of properties of bio-oil in comparison with diesel and gasoline

	<b>Bio-oil</b>	<b>Diesel</b>	<b>Gasoline</b>
H/C ratio	1.2-1.4	2	1-2
O/C ratio	0.5	0	0
Carbon chain length	Up to 100	12-20 alkanes (linear)	Aromatics, 5-10 branched alkanes

### 2.6.3. Pyrolysis Mechanism

The bio-oil is derived from pyrolysis through a series of dehydration, repolymerization, depolymerization and fragmentation reactions of lignin, cellulose and hemicellulose. Owing to complex composition of biomass, the reaction mechanisms are not completely understood. The properties of bio-oil are varied with type of feedstock, process operating conditions and type of pyrolysis process employed. Heating of biomass in oxygen free environment leads to scission of chemical bonds within the polymers. As a result, volatile species are released. Conversion of biomass primarily follows three pathways, frequently termed as fragmentation, char formation and depolymerization (Dickerson et al., 2013).

#### i. Depolymerization

In depolymerization, chemical bonds between monomers units are broken down that leads to the production of volatile molecules. These molecules are then condensed and found in bio-oil as monomers, dimers or trimer (Collard et al., 2014).

#### ii. Fragmentation

In this mechanism, covalent bonds of polymers are linked together, which results in the formation of gases and small chain organic species (Collard et al., 2014).

### iii. Char formation

This mechanism results in the formation of solids referred to as bio-char. Biochar represents an aromatic polycyclic structure. This occurs due to intra and intermolecular rearrangement reactions leading to high degree of reticulation (Collard et al., 2014).

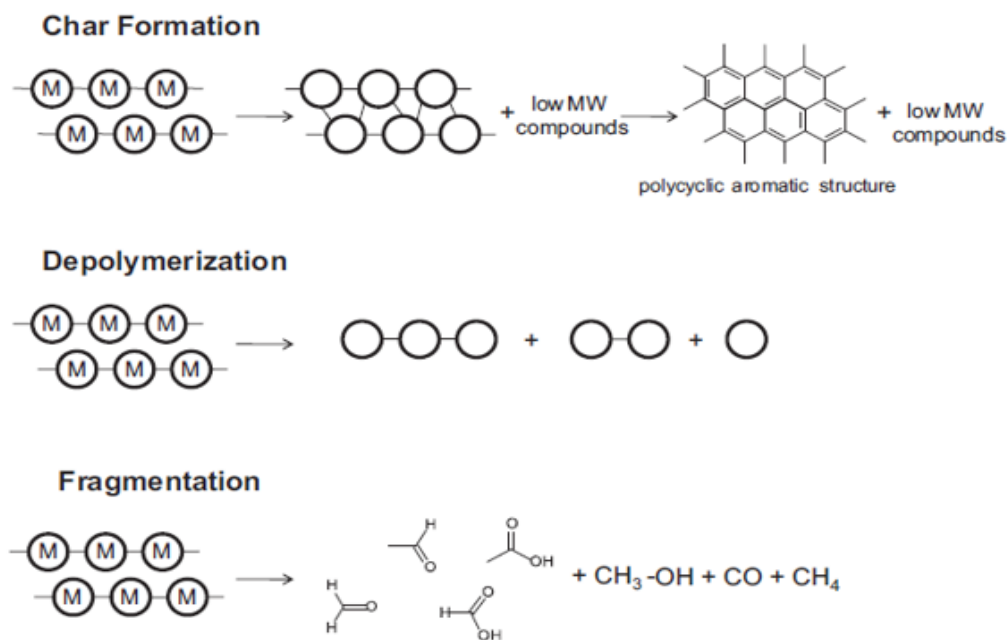


Figure 2.5: Pathways involved in conversion of biomass during pyrolysis

#### 2.6.4. Factor affecting pyrolysis process

The product yield of pyrolysis process is influenced by different process variables i.e. type of reactor, temperature, sweeping gas flow rate, biomass heating rate, biomass type, size of feedstock particles etc.(Akhtar et al., 2012).

##### 2.6.4.1. Temperature

Temperature is an important operating parameter that provide required heat of decomposition to fragment linkages within biomass particles. Bio-oil yield and composition vary significantly with change in reaction temperature. Low reaction temperature (<300°C) favors the production of heavy tars while high temperature i.e. (around 550°C) leads to massive fragmentation of biomass bonds resulting in higher

liquid oil yields. Increasing temperatures beyond 600°C augment gas products yields due to secondary cracking reactions. Based on extensive researches, it has been concluded that temperature in 500-550°C range maximizes liquid product yield for various biomass feedstock (Akhtar et al., 2012).

#### 2.6.4.2. Biomass heating rate

Pyrolysis process can be classified as slow, intermediate or fast pyrolysis depending upon heating rate and vapor residence time. Essential features of slow pyrolysis are very slow heating rate, lower temperature (400 °C) and longer vapor residence time. Slow pyrolysis usually takes hours to complete process and favors the production of biochar with concurrent increase in water content of bio-oil. Intermediate pyrolysis employs relatively higher heating rate and vapor residence time of 10-20 seconds. In fast pyrolysis, biomass is heated very rapidly and vapors residence time is less than 2 seconds. High heating rate and rapid quenching of pyrolysis vapors avoids repolymerization reactions of decomposed molecules (Akhtar et al., 2012). Fast pyrolysis maximizes production of bio-oil and may yield up to 70-80% of feedstock and takes seconds to complete the process (Bulushev et al., 2011). All three modes of pyrolysis yield different proportions of pyrolysis products, shown in table below.

Table 2.2: Modes of Pyrolysis process w.r.t. heating rates

Mode of pyrolysis	Residence time (Sec)	Temperature (°C)	Yields (wt.%)		
			Biochar	Bio-oil	Gas
<b>Fast</b>	<2	500	12	75 (25% water)	13
<b>Intermediate</b>	10-20	500	25	50 (50% water)	25
<b>Slow</b>	Very long	400	35	30 (70% water)	35

#### 2.6.4.3. Biomass type

Being non-selective, pyrolysis process can convert a wide range of lignocellulosic biomass to desirable end products. The economics of pyrolysis' feedstock is generally considered advantageous for biomass resources that are cheap, locally available, require less land for cultivation and/or present as waste (S. Liu et al., 2017). Substantial quantities of waste biomass present a potential feedstock for pyrolysis

without any additional land use. Waste biomass from forest include tree bark, the loggings, debris from site clearing, scrap wood etc. Crop processing produces substantial quantities of agricultural residues in the form of straw, stack, husk etc. Examples of agricultural residues are wheat straw, sugarcane bagasse, rice straw, corn straw, olive pits, tobacco stalks and nut shells etc. Based on 2012 estimate, 1394 million tons of agricultural residues are available globally (Kabir et al., 2017).

Table 2.3: Pyrolysis products obtained from different types of feedstocks.

Feedstock type		Temp °C	Yield (wt. %)			Ref
			Bio-oil	Char	Gas	
Woody biomass	Eucalyptus wood	450	60.5	21.5	18	Kumar et al. (2010)
	Poplar bark	475	63.3	20.5	16.2	Iliopoulou et al. (2012)
	Pinewood	450	32.7	15.3	52	Aho et al. (2008)
Agricultural residues/wastes	Sugarcane bagasse	560	53.4	25.31	18.31	Mantilla et al. (2014)
	Wheat Straw	500	35	33	32	Farooq et al. (2018b)
	Rice straw	550	30	27	15	Pütün et al. (2004)
	Sesame stalk	550	56.2	19.5	24.28	Ateş et al. (2004)
	Corn stalk	500	52	20.5	27.5	Uzun et al. (2009)
	Sunflower bagasse	550	46	26	28	A. Pütün et al. (1996)
	Cotton stalk	500	38	27	35	Shah et al. (2019)
	Olive bagasse	500	37.7	31.8	30.5	Şensöz et al. (2006)
Municipal & Industrial waste	Palm empty fruit bunch	540	48.4	29.63	17.84	Mantilla et al. (2014)
Energy crops	Rape seed	550	70	14	16	Onay et al. (2001)
	Euphorbia Rigida	550	42	12	46	A. E. Pütün et al. (1996)
Aquatic Plants (Microalgae)	C. Protothecoides	500	17.5	52	30.5	Miao et al. (2004)
	M. aeruginosa	500	23.7	21	55.3	Miao et al. (2004)

#### 2.6.4.4. Sweep Gas flow rate

The type and composition of pyrolysis' products is highly influenced by reaction environment. The escaped volatiles from pyrolysis react either with surrounding solids thus provoke char formation or further crack to lighter gases in secondary reactions. Therefore, rapid quenching of primary vapors from reaction environment is essential which is accomplished by using a constant flow rate of gases e.g. Ar, N<sub>2</sub>, He etc. It is

reported that augment in gas flow rate from 50ml/min to 200ml/min enhanced liquid yield by 3%. However, very high sweeping rate results in lower liquid yield due to insufficient condensation system. (Akhtar et al., 2012).

#### **2.6.4.5. Types of pyrolysis reactors**

Reactor is considered as the heart of pyrolysis process. Various reactor configurations have been developed and tested by academic institutions over last few years in order to optimize pyrolysis process. Reactor design is focused on improving desirable conditions such as short vapor residence time, moderate temperature and rapid heating rate. However, each type of reactor has its own limitations, advantages and maximum yielding capacity of bio-oil (Bridgwater et al., 2012; Jahirul et al., 2012). The most commonly employed reactor types are described in following sections.

##### **i. Fixed Bed Reactor**

Fixed bed system consists of a reactor usually made up of steel or concrete. This reactor has a feedstock feeding unit, sweeping gas inlet, a gas exit and char removal system. Fixed bed reactor is generally characterized by long reaction time, low bio-char carryover and low gas velocity. This type of system is reliable for uniform sized feedstock and low fines content. Fixed bed reactor is likely to give low bio-oil yield with phase separated products.

##### **ii. Fluidized-Bed Reactor**

In fluidized bed reactor, a pressurized fluid is introduced into system and passed through feedstock particles providing high surface contact between fluid and solid particles. This type of system is popular for fast pyrolysis as it provides an efficient temperature control and heat transfer to feedstock particles and high gas velocity. Two types of fluidized bed reactor are bubbling fluidized bed reactor and circulating fluidized bed reactor.

##### **iii. Ablative Reactor**

In this type of reactor, biomass is mechanically pressed against hot wall of reactors which results in melting of biomass particles. As biomass melts, it moves away from wall and evaporated. ablative reactor has the advantage of using larger biomass particles i.e. up to 20 mm in contrast other reactors which significantly requires very small sized (<2mm) biomass thus reducing costs associated with grinding. However, mechanical nature of this process makes this configuration a little bit complex. Examples of ablative reactor are vortex reactor and rotating disc reactor. In ablative reactors there is no requirement of inert gas .

#### **iv. Microwave Reactor**

In microwave reactor type, heat transfer is accomplished by interaction of biomass particles and microwave heated bed. Microwave oven is driven by electricity. Eddy current are generated which provide fast heating. Feedstock is placed within microwave cavity and particles are heated within source not by external heating source. Eddy Oxygen free atmosphere is created using an inert gas which also act as carrier of volatiles.

#### **v. Auger Reactor**

This type of reactor utilizes augurs to move the biomass mechanically through a heated cylinder which is kept at desired pyrolysis temperature. This reactor does not employ fluids. Biomass is exposed to high temperature which cause it to volatilize instantly. An important feature of this type of reactor is that vapor residence time can be varied by changing heated zone through which vapor are passed before condensation.

#### **vi. Solar Reactor**

Solar reactors are capable of storing solar energy into chemical energy. Solar reactors are commonly made up of quartz tube having an opaque external surface which is exposed to solar radiations. Solar radiations are concentrated with the help of parabolic solar concentrator and are capable of creating high temperature within reactor.

Solar reactor utilizes renewable source of energy for heating thus making the pyrolysis process energy efficient.

#### **vii. Vacuum Pyrolysis Reactor**

In this type of reactor, vacuum is created within the reactor and biomass is introduced into high temperature zone which is mechanically agitated. Vacuum pyrolysis reactor is not preferable for fast pyrolysis due to heat transfer limitations. Heat transfer rate to biomass and through biomass is much lower as compared to other reactor configurations. This leads 35-50% to bio-oil yields in contrast to 75% as achieved by fluidized bed configurations. The main advantage of vacuum reactor is that it can be operated using larger sized biomass (2-5cm).

#### **2.6.5. Drawbacks of bio-oil**

Bio-oil is a heterogenous blend, containing wide spectrum of organic species with molecular weights ranging from 18-5000g/mol (Sebestyén et al., 2017). Poor selectivity of conventional pyrolysis process results in more than 300 different types of organic compounds in bio-oil (Lu et al., 2017). Crude bio-oil experiences certain undesirable properties such as low calorific value, high oxygen content (30-40 wt%) and water content, high viscosity and density, corrosive nature, thermal instability during storage, extreme ignition delay and incomplete volatility (H. Hassan et al., 2016; Iliopoulou et al., 2012).

These detrimental characteristics are mainly due to the presence of several classes of oxygenated organic species such as ketones, aldehydes, acids, alcohols and ethers (H. Hassan et al., 2016). These oxygenated compounds increase O/C of bio-oil (0.5, approximately) higher than that of petroleum fuels. High oxygen content reduces its calorific value to almost half of the conventional fossil fuels. Calorific values reported for several feedstocks is in range of 16 - 19 MJ/kg (Bulushev et al., 2011).

Presence of acids mostly acetic and formic acids reduce pH value (2–3) leading to corrosiveness. Ketones compounds cause instability. Ester species are responsible for



low heating values of bio-oil. Nitrogen compounds present environmental concerns. Presence of suspended particles may adversely affect combustion process as they may get plugged in equipment nozzles (Dickerson et al., 2013). High moisture content in bio-oil reduces the flame temperature during combustion (Gollakota et al., 2016).

Bio-oil ages with time due to slow polymerization reactions resulting in variable viscosity i.e. in range of 10 to 10,000 cp. Aging process is accelerated when exposed to light, oxygen or temperature higher than 80 °C leading to storage problems (Dickerson et al., 2013). Higher viscosity engenders high-pressure drop in pipe lines during transportation resulting in higher maintenance of equipment. Moreover, higher amount of energy is required to reheat the bio-oil during up gradation. (Gollakota et al., 2016; Huang et al., 2015).

#### **2.6.6. Upgradation of un-processed bio-oil**

All these characteristics render the bio-oil incompatible with standard petroleum-based refineries. In order to make bio-oil equivalent to customary petroleum fuel and economically attractive it is inevitable to upgrade bio-oil (Carpenter et al., 2014). The focal objective of upgradation process is to eliminate reactive oxygenated compounds and cracking of large molecular structures to smaller one thus improving energy density of bio-oil (Bulushev et al., 2011; Gollakota et al., 2016). Upgraded bio-oil can be utilized

- As Combustion fuel
- Directly as transportation fuel
- As drop-in feedstock in existing petroleum-based infrastructure
- In power plant for energy production
- In production of chemicals and resins
- For production of anhydro-sugars e.g. levoglucosan
- In diesel fueled engine by blending with diesel oil

## **2.7. Upgradation methods**

Crude bio-oil can be upgraded to valuable fuel that resembles to petrochemical products. Several efforts have been made to upgrade bio-oil either by altering pyrolysis process referred to as “insitu upgradation” or upgrading bio-oil through additional treatments (Güngör et al., 2012). In this respect, various mechanisms such as hydrodeoxygenation, catalytic upgrading, esterification, steam reforming, super critical extraction, emulsification etc. have been reported in literature. (Gollakota et al., 2016)

### **2.7.1. Catalytic upgradation**

Thermo-catalytic pyrolysis has been realized as a robust method in order to obtain upgraded oil (Iliopoulou et al., 2012). Application of heterogeneous catalyst in pyrolysis process with the purpose to expel the reactive oxygenated compounds seems to be most pragmatic (Mihalcik et al., 2011). Catalytic upgrading is intended to reduce reaction temperature leading to scission of high molecular weight organic compounds to lighter ones and less oxygenated hydrocarbons. Moreover, the selective nature of a specific catalyst may help to attain desirable products like aromatics and olefins (Botas et al., 2012). Catalytic pyrolysis aids in eliminating secondary reactions during storage of bio-oil (Xue et al., 2016).

During catalytic upgradation, oxygen from polar groups is rejected in the form of CO and CO<sub>2</sub> at higher temperatures and H<sub>2</sub>O at lower temperature. Removal of O<sub>2</sub> in the form of CO<sub>2</sub> is more preferable as compared to CO because only one carbon atom is consumed in removing two oxygen atoms thus increasing H/C of bio-oil. Rejection of oxygen in the form of water is least desirable as it leads to elimination of two hydrogen atoms that must be incorporated in hydrocarbon forming reactions (Lappas et al., 2012). It should be noted that quality of upgraded oil not only depends upon reduced oxygen content but also on the types of remaining functional groups. For example, phenol is an oxygenated chemical compound but presence of acids is more detrimental in oil. Therefore, oxygen functionalities must be steered to acceptable products e.g. ether, alcohols, and phenols (Carpenter et al., 2014; Dutta et al., 2015).

### 2.7.1.1. Cracking mechanism

Catalyst can significantly alter the bio-oil's yield and composition thus effecting its physical and chemical characteristics. In catalytic pyrolysis, primary products from thermal degradation of biomass undergo a suite of cracking, deoxygenation and reforming reactions (Yildiz et al., 2016). Deoxygenation is mainly accomplished by decarbonylation, decarboxylation, dehydration and aromatization reactions occurring simultaneously within structure of catalysts (French et al., 2010). The reaction pathways are mainly dependent on reaction mode, feedstock type, catalyst type and other operating conditions during catalytic pyrolysis (Rahman et al., 2018).

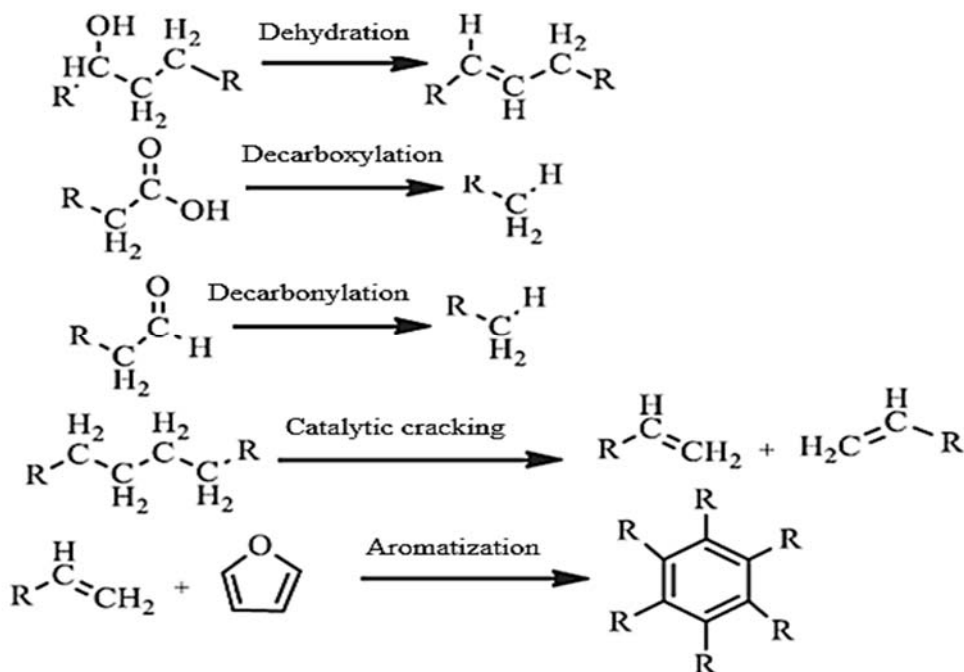


Figure 2.6: Mechanisms involved in catalytic cracking, Adapted from (Rahman et al., 2018)

### 2.7.1.2. Types of catalyst

A plethora of heterogenous catalysts such as mesoporous zeolites (MCM-41, SBA-15, MSU), microporous zeolites (ZSM-5), metal oxides (MgO, CaO,  $\text{TiO}_2$ ,  $\text{Fe}_2\text{O}_3$ , NiO and ZnO etc.) and catalysts doped with transition (Zn, Co, Ni, Fe, Cu) and noble metals (Ag, Au, Pt) have been investigated in an attempt to upgrade bio-oil (Rahman et al., 2018). An ideal catalyst is cheap, strong, supposed to produce high yield as well as

high quality (higher octane number products) of bio-oil, exhibiting long catalytic life and thermal stability. It should inhibit production of undesirable organic compounds such as ketones, acids, carbonyl compounds which render the bio-oil incompatible with standard petroleum-based refineries (Botas et al., 2012; Lappas et al., 2012) .

Catalytic pyrolysis of olive residue was performed using synthetic (ZSM-5) and natural zeolite (NZ). They reported that the bio-oil yield for natural catalyst was higher than that of synthetic. Cracking over ZSM-5 increased the gas production at the expense of bio-oil yield. Augment in catalyst to feedstock ratio increases gas products, bio-char and coke. However, the use of ZSM-5 favored the production of lighter hydrocarbons, aromatic compounds and reduction in polar groups resulting in increased heating value of upgraded oil (Pütün et al., 2009). Kim et al. (2015) have compared the performance of three types of zeolites i.e. HZSM-5, HBETA, Al-MCM-41 using Tandem  $\mu$  reactor - GC-MS. Results proved that HZSM-5 is highly selective toward formation of aromatics. Aromatic yield over HBETA was slightly higher than HZSM-5 but produced more polyaromatic hydrocarbons (PAH) which are precursors to coke formation.

Catalytic pyrolysis of pinewood was conducted using four different types of acidic zeolites i.e H-Beta-25, H-Y-12, H-ZSM-5 and H-MOR-20 in order to determine effect of zeolite structure. All four zeolites slightly influenced products yield and maximum yield was obtained by H-ZSM-5, almost equivalent to non-catalytic bio-oil but with high water content. Chemical composition of bio-oil obtained over H-Beta-25, H-Y-12, and H-MOR-20 elucidated almost same types of chemical groups. H-ZSM-5 discouraged the production of acids and alcohols but favored production of ketones. H-MOR-20 produced smaller fraction of poly aromatic hydrocarbons. In the same study, it was concluded that spent catalyst can be regenerated without altering its chemical structure. In view of the studies reported above and in table 2.4, it can be concluded that ZSM-5 is the promising catalyst capable of reducing oxygenated content of bio-oil and producing large aromatic fractions in bio-oil which can be used as fuel.

Table 2.4: Use of different catalysts in upgradation

Feedstock	Catalyst	Reactor configuration	C/F	Mode	Type & Heating rate	Flow rate	Temp. Pyrolysis Catalytic	Findings	Ref.
					°C/min		ml/min		
<b>Type of catalyst</b>									
Empty fruit bunches	HZSM-5, bentonite, dolomite, olivine, spent FCC catalyst	Fixed bed Reactor	1	In-situ	Fast -	-	500	Maximum (40.4 %) aromatics by HZSM-5	Ro et al. (2018)
Rapeseed cake	Na <sub>2</sub> CO <sub>3</sub> , HZSM-5, -Al <sub>2</sub> O <sub>3</sub>	Fixed bed Reactor	0.47	Ex-situ	Slow -	50	550 -	14% wt. deoxygenation for HZSM-5. HZSM-5 zeolite showed the highest liquid yield (44.9 wt.%)	Smets et al. (2013)
Wood biomass	ZSM-5, MgO, Alumina, Titania, Zirconia/Titania, Silica alumina	Fixed bed Reactor	0.5	In-situ	Fast -	100	500 -	zirconia/titania & ZSM-5 gave organic liquid with reduced oxygen content and higher aromatics content	Stefanidis et al. (2011)
<b>Mode of cracking</b>									
Corn stalk	ZSM-5, H-Y and USY	Fixed bed Reactor	-	Ex-situ In-situ	Fast 500	400	500 -	Optimum bio-oil by ZSM-5 USY enhanced aromatics H-Y increased aliphatic	Uzun et al. (2009)
Pine bark	ReUS-Y, red mud and ZSM-5.	Fixed bed reactor		Ex-situ In-situ	Slow 7	25	400-700 -	ZSM-5 and ReUS-Y decreased in O <sub>2</sub> content while red mud increased H <sub>2</sub> O formation	Güngör et al. (2012)
<b>C/F variation</b>									
Olive residue	H-Y, ZSM-5, Clinoptilolite	Fixed bed Reactor	0.05,0.1, 0.15,0.2, 0.25	Ex-situ	Fast 500°	-	500 400	Optimum C/F is 0.2, 0.1, 0.05 for NZ, ZSM-5, H-Y respectively	Pütün et al. (2009)
<b>Catalytic temperature variation</b>									
Citrus-unshiu peel, wood powder	HZSM-5, HBETA, Al-MCM-41	Tandem $\mu$ reactor - GC-MS	1:01	Exsitu	Fast -	-	500 400,500,600	Aromatic yield over HBETA (9.69 C%) , HZSM-5 (6.78 C%). HBETA produced more MAH	Kim et al. (2015)

### 2.7.1.3. Zeolite ZSM-5

Zeolite has received increasing attention due to its low price, massive availability and facile tunability. The extensive research in catalyst screening and design has elucidated the zeolite ZSM-5 (Zeolite Socony Mobil-5), a highly effective and promising catalyst in terms of its strong ability of deoxygenation and shape selectivity. It can effectively acts as cracking catalyst under atmospheric conditions without addition of pressurized hydrogen gas resulting in reduction of operating cost (Pütün et al., 2009).

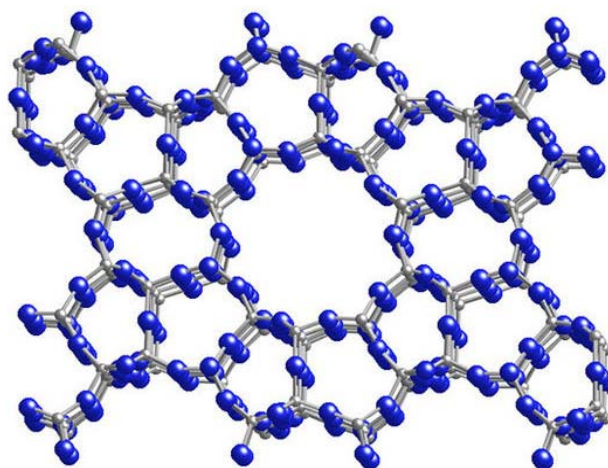


Figure 2.7: 3D structure of HZSM-5

ZSM-5 zeolite is characterized by three-dimensional crystalline structure having interconnected network of channels (Zig Zag and linear), intermediate pore size (0.52-0.56 nm), better acidity, higher resistance to deactivation. Micropores of ZSM-5 allow to enter small molecules which are then folded to aromatics (Botas et al., 2012; Pütün et al., 2009). Cracking of pyrolysis vapors over ZSM-5 gives high yield of aromatic compounds which can be further upgraded to diesel and gasoline type fuels (Iliopoulou et al., 2012).

Catalytic effect of HZSM-5 for cracking of pyrolysis vapors from different biomasses and model compounds has been investigated extensively. ZSM-5 has been used to transform oxygenated organic compounds to hydrocarbons since late 1970s. Initially it was used by Mobil for effective conversion of methanol to diesel range

fuel (French et al., 2010). It has been reported that ZSM-5 can lessen oxygen content from 33% to 13 % (Rahman et al., 2018).

#### **2.7.1.4. Factors affecting pyrolysis over ZSM-5**

Process parameters that must be considered during catalytic pyrolysis include temperature, biomass heating rate, catalyst to feedstock ratio. These parameters are known to influence the yield as well as chemical composition of the products (Yildiz et al., 2016).

##### **2.7.1.4.1. Pyrolysis temperature**

Temperature provides required heat of decomposition to fragment linkages within biomass particles. Bio-oil yield and composition vary significantly with change in reaction temperature. Wang et al. (2016) have investigated the potential of HZSM-5 in slow pyrolysis of pine using two stage fixed bed reactor. The results showed 14.5–16.8% of bio-oil yield at 550–600 °C with high heating values of 39.1–42.4 MJ/kg. Mendes et al. (2016) investigated the effect of different reaction temperatures i.e.450-550°C in catalytic pyrolysis of sugarcane bagasse and pinewood over ZSM-5. The study revealed that gas yield increased with increase in temperature however coke yield was reduced. Maximum liquid yield for both feedstocks was attained at 500°C. In addition to temperature effect, ZSM-5 presence enhanced gas yield by promoting deoxygenation reactions.

##### **2.7.1.4.2. Catalyst to feedstock ratio**

Catalyst to feedstock ratio is an important operating parameter in catalytic pyrolysis of biomass. Muley et al. (2015) attempted to upgrade of pinewood sawdust pyrolysis vapors over HZSM-5 at different catalyst to feedstock (C/F) ratio (1,1.5,2) and catalytic temperatures (290°C,330°C,370°C). It was reported that with increase in catalytic temperature and C/F, quality of bio-oil is improved with highest aromatic yield of 32.02% was at C/F of 2. S. Liu et al. (2017) showed that liquid yield decreased while aromatic yield increased with augment in C/F. Lazaridis et al. (2018) valorized lignin in the presence of ZSM-5 having different porosity and acid characteristics. In this study, C/F was varied from 1-4. It was shown that higher C/F triggered the conversion of alkyl phenol toward mono aromatics and PAH.

Ghorbannezhad et al. (2018) varied C/F from 2-23 during pyrolysis of sugarcane bagasse over HZSM-5. Maximum liquid yield was obtained at C/F of 12.5.

#### **2.7.1.4.3. Mode of cracking**

Catalysts could be employed in pyrolysis process in number of configurations; they could be directly mixed with biomass feedstock in pyrolysis vicinity referred to as in-situ pyrolysis, could be applied downstream of pyrolysis reactor commonly known as ex-situ pyrolysis or could be used to upgrade condensed bio-oil. In insitu pyrolysis mode, catalyst temperature is same as the pyrolysis reaction temperature and vapors from pyrolysis come in contact with catalyst immediately after their formation and upgraded within the reactor. In ex-situ mode of pyrolysis, catalytic temperature could be independently controlled and vapor phase is upgraded in a separate reactor (Yildiz et al., 2016). Iisa et al. (2016) have compared the exsitu and Insitu catalytic pyrolysis of pine in a fluidized bed reactor using ZSM-5 at 500 °C. This study revealed that insitu configuration produced slightly higher bio- oil yield but with more oxygen content as compared to exsitu configuration, showing rapid catalyst deactivation in Insitu mode. Over all, organic mass yield was in range of 16-18% with almost 45% reduction in oxygen content.

#### **2.7.1.4.4. Catalytic temperature**

The temperature of catalyst is one of major process parameters when catalyst is employed outside the vicinity of pyrolysis reactions i.e. exsitu pyrolysis. Huang et al. (2015) converted pine sawdust pyrolyzates to advanced bio-fuel using HZSM-5. Three different catalytic temperatures were evaluated to determine upgradation potential of HZSM-5. It was noted that highest hydrocarbon yield (58.63%) and C<sub>8</sub>-C<sub>12</sub> (48.03%) was obtained at 500°C (both catalytic and pyrolysis). The high heating value of upgraded oil was 23 MJ/Kg higher as compared to of pine sawdust i.e. 19 MJ/Kg. S. Liu et al. (2017) have assessed the performance of HZSM-5 in sequential microwave assisted pyrolysis of corn stover followed by packed bed catalysis. The effect of catalyst bed temperature and pyrolysis temperature was evaluated. It was elucidated that catalyst bed temperature significantly affect the aromatic content in bio-oil with maximum 26.2% aromatics found at 425°C. Moreover, coke yield decreased with increase in catalytic temperature.



Table 2.5: Use of HZSM-5 for catalytic upgrading

Feedstock	Catalyst type	Reactor configuration	C/F	Mode	Type & Heating rate	Flow rate	Temp. Pyrolysis Catalytic		Findings	Ref.
					°C/min		ml/min	°C		
Pine sawdust	HZSM-5	fluidized-bed / fixed-bed combination	7.5	ex-situ	Fast -	1000	550 600		Aromatic + olefins (21.7%)	Hu et al. (2017)
Pinewood	HZSM-5	Fixed bed Reactor	~3	ex-situ	Slow 10	200	550-600	550	16.8% bio-oil yield with 42.4 Mj/kg HHV, 33-35% Energy recovery	Wang et al. (2016)
Sugarcane bagasse	HZSM-5 (SAR:23, 50, 80)	Tandem micro reactor-GC/MS	2-23	ex-situ	Fast -	-	400,450,500,550 450		Max BTEX yield (22%) over HZSM-5 (23) was obtained at temperature of 475°C, C/F of 12.5	Ghorbannezhad et al. (2018)
Yellow pine	A: HZSM-5 (12% bentonite) B: HZSM-5 (20% SiO <sub>2</sub> )	Fluidized Bed Reactor	A:0.17 B:0.13 B:0.11	in-situ in-situ ex-situ	Fast -	14000	500	500	Bio-oil yield :17.3 wt.% Bio-oil yield 16.9 wt.% Bio-oil yield 14.1 wt.%	Iisa et al. (2016)
Pinewood sawdust	HZSM-5	Fixed bed with induction heating	1:1, 1.5:1, 2:1	ex-situ	Fast -	1000	600 290,330,370		32.02% aromatics with C/F:2:1 (optimum)	Muley et al. (2015)
Sewage sludge	HZSM-5	Tandem micro-reactor	20	ex-situ	Fast -	90	400-800(600ct) 400-800(500pt)		Optimal pyrolysis & catalytic temperature were 500 & 600°C respectively	K. Wang et al. (2017)
Pine sawdust	HZSM-5	Fixed bed Reactor	0.1	ex-situ	Slow 20	3	500 400,500,600		HC Content (58.63%), C8-C12 carbon content (48.03%), upgraded oil of 23Mj/kg	Huang et al. (2015)

\*ct: catalytic temperature, pt: pyrolysis temperature

#### **2.7.1.5. Challenges in cracking over ZSM-5**

A major drawback associated with thermo-catalytic upgrading over ZSM-5 is coke deposition. Coke is defined as carbonaceous material formed resulting from heterogeneous reactions of pyrolytic vapors. Coke deposited over catalyst results in catalyst deactivation (Li et al., 2013). Frequent regeneration shortens the catalyst's service life as high risks of sintering are associated with successive regeneration. This impedes the use of ZSM-5 as commercial catalyst in industry (Muley et al., 2015). ZSM-5 is highly acidic in nature. This is advantageous in terms of producing high yields of aromatic products. However high acidity results in severe cracking of vapors toward non-condensable gases and higher amount of coke is deposited over catalyst, thus reducing organic product yield (12-15% hydrocarbons) and increasing water content of bio-oil. Bio-oil yield follows an inverse trend with better quality. High amount of water content may be attributed to pronounced dehydration reactions in the presence of catalyst (Hu et al., 2017). Polymerized and dehydrated/ dehydrogenated compounds from pyrolytic vapors are responsible for coke deposition (Kantarelis et al., 2014).

Formation of coke leads to deprivation of carbon in bio-oil. Furthermore, production of higher amount of polycyclic aromatic hydrocarbons (PAHs) and lower amount of monocyclic aromatic hydrocarbons (MAHs) have been reported with unmodified ZSM-5. Fluorene and anthracene i.e. polyaromatic hydrocarbons, are commonly considered as coke precursors (Fanchiang et al., 2012). These PAHs are not environment friendly and known to be carcinogenic/mutagenic. Low carbon yield obtained in catalytic cracking makes impractical to scale up catalytic pyrolysis process in bio-oil based refineries.

#### **2.7.1.6. H/C<sub>eff</sub> ratio**

Hydrogen to carbon effective ratio plays an important role in coke formation and in effective conversion of pyrolysis products to acceptable fuels. This ratio indicates the relative content of hydrogen in feedstock.

$$\frac{H}{C_{\text{eff}}} = \frac{H-2O-3N-2S}{C}$$

Where C, H, O, N, S are moles of carbon, hydrogen, oxygen, nitrogen and sulfur respectively, present in feedstock. The petroleum feedstock has  $H/C_{\text{eff}}$  greater than 1 e.g. benzene and butane have value of 1 and 2.5 respectively. Biomass is deficient in hydrogen i.e.  $H/C_{\text{eff}}$  is usually less than 0.3 (Zhang et al., 2015).  $H/C_{\text{eff}}$  of some biomasses used for pyrolysis are given in table below.

Table 2.6: Effective hydrogen to carbon ratio of different biomasses

<b>Biomass</b>	<b>C</b>	<b>H</b>	<b>O</b>	<b>N</b>	<b>S</b>	<b>H/C<sub>eff</sub></b>	<b>Ref.</b>
Citrus unshiu peel	42.9	6.4	46.4	1	-	0.108	Kim et al. (2015)
Wood powder	45.3	6	43.4	3.2	-	<0	Kim et al. (2015)
Olive residue	49.08	5.59	44.19	1.14	-	<0	Pütün et al. (2009)
Empty fruit bunches	42.6	5.7	39.5	1.7	0.3	0.106	Ro et al. (2018)
Pine sawdust	44.2	5	49.7	1.1	-	<0	Hu et al. (2017)
Beech wood	45.98	6.39	46.28	-	-	0.158	Iliopoulou et al. (2012)
Sugarcane bagasse	48.9	6.1	44.78	0.22	-	0.111	Huang et al. (2012)
Rice husk	44.9	6.35	48.3	0.45	-	0.057	Huang et al. (2012)
Sawdust	46.2	6.02	47.3	0.48	-	0.001	Huang et al. (2012)
Jatropha residues	49.2	6.4	39.6	4.5	1.1	0.10	Vichaphund et al. (2015)

Previous studies have revealed that there is a strong correlation between  $H/C_{\text{eff}}$  of biomass and biomass-derived hydrocarbons (Zhang et al., 2015). It is discerned that coke formation is primarily associated with low hydrogen content of lignocellulosic biomass (Zhang et al., 2016). Thermal decomposition of biomass engenders large number of oxygenated compounds e.g. acetic acids, acetone etc. These oxygenates due to low  $H/C_{\text{eff}}$  are converted to coke precursors over catalyst. The major challenge in catalytic pyrolysis of biomass is to minimize coke formation, is a Therefore, there is need to introduce hydrogen sources either by direct injecting hydrogen gas or by modifying reaction environment. Introduction of molecular hydrogen is not cost-effective method. Alcohols ( $H/C_{\text{eff}} = 1.5$ ) and grease ( $H/C_{\text{eff}} = 2$ ) could be added as a hydrogen source to improve yield of desirable products, however high prices of these

co-reactant make impractical to use them (Zhang et al., 2015). Therefore, this objective can be garnered via two relatively low-cost methods i.e.

- Modification of acidic ZSM-5 catalyst
- Incorporation of a hydrogen donor co-reactant

#### **2.7.1.7. ZSM-5 modification**

Acid sites and porosity of ZSM-5 zeolite must be tailored in an effort to develop an optimized catalyst. Modified catalyst must exhibit the following features and/or functions;

- Long catalyst service life through reduction in coke and coke precursors formation
- Higher carbon efficiency of products due to enhanced hydrodeoxygenation reactions
- Reduction in gaseous products and more formation of distillate range hydrocarbons, thus improving organic yield
- Removal of oxygen from oxygenated compounds preferably by CO<sub>2</sub> instead of CO
- Higher selectivity toward monocyclic aromatic hydrocarbon

#### **2.7.1.8. Metal modified ZSM-5**

Increasing attention is now being paid to modify ZSM-5/ HZSM-5 by incorporation of metals within catalyst structure. Promotion of ZSM-5 with different metals such as, Lead, Nickel, Cobalt, Iron, Gallium, Tin, Zinc, Cerium etc. have been reported in literature (S. Zhang et al., 2018). Metal modified ZSM-5 has been realized as an efficient candidate with selective deoxygenation potential. Incorporation of transition metals is suggested to affect the mechanism of oxygen removal in a way that it rejects oxygen more in the form of carbon oxides instead of water, thus provides more hydrogen available for hydrocarbon production (French et al., 2010).

Modified catalyst produce hydrogen through WGS reaction (Kantarelis et al., 2014). It has been confirmed that modification of ZSM-5 with metals alter acid site and textural properties of catalyst (Botas et al., 2012). This is helpful in attenuating rate of coke formation over catalyst and improve liquid product yield. ZSM-5 doped with metals was also considered to improve hydrothermal stability of the catalyst. Adequate stability of catalyst is very important in successive reaction and regeneration steps (Iliopoulou et al., 2012). Addition of metals in ZSM-5 decreases concentration of Brønsted acid sites and generates additional Lewis acid sites (Rahman et al., 2018). Thus, formation of new active sites over ZSM-5 inhibit repolymerization of MAH and promotes aromatization reactions resulting in enhanced selectivity toward BTEX (Iliopoulou et al., 2014).

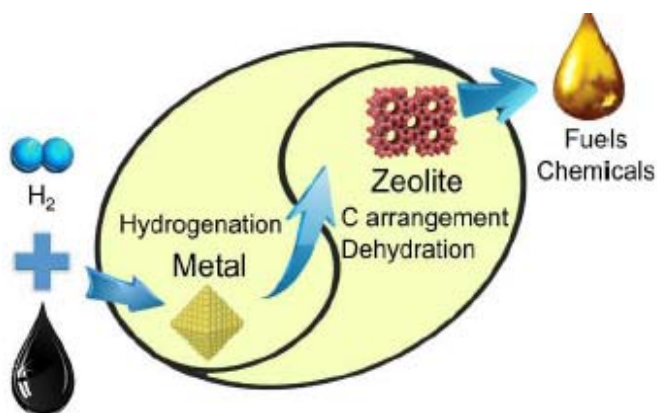


Figure 2.8: Cracking mechanism of bi-functional catalyst

French et al. (2010) have evaluated the catalytic effect of metal (Co, Fe, Ni, Ce, Ga, Cu, Na) modified ZSM-5 in pyrolysis of cellulose, lignin (model compounds) and wood using a microreactor system coupled with Molecular-beam mass spectrometry (MBMS). ZSM-5 modified with Ni, Co, Fe, Ga produced high hydrocarbon yield while highest hydrocarbon yield was achieved by nickel substituted ZSM-5 i.e. 16 wt.%. In the same study, semi-continuous flow reactor was employed to assess the cracking and deoxygenating potential of catalyst as a function of the catalyst time-on-stream. It was reported that, with increase in catalyst time-on-stream, deoxygenation activity was reduced which is possibly due to formation of coke over catalyst. Iliopoulou et al. (2012) have assessed the performance of commercial diluted ZSM-5 doped with Ni and Co

transition metals. Metals loading on ZSM-5 support was varied from 1-10 %. Metals were in oxide form i.e. NiO and Co<sub>3</sub>O<sub>4</sub>. Results showed that NiO is more reactive compared to Co<sub>3</sub>O<sub>4</sub> and decreased organic phase of bio-oil and increased gaseous product. However, both metals substituted catalyst exhibited less dehydration activity and more selectivity toward aromatics and phenols. Oxygen content of organic phase was reduced markedly by both catalysts.

Fanchiang et al. (2012) have conducted pyrolysis of furfural (a model compound of cellulose) using HZSM-5 and Zn/HZSM-5 in continuous fixed bed system. Impact of reaction temperature (300 °C, 400 °C, 500 °C), metal loading (0.5 & 1.5 %) and vapor contact time on product distribution were evaluated. Anchored ZnO in Zn/H-ZSM5 has shown a significant role in hydrogen transfer reactions. This can be attributed to modification of acid sites of H-ZSM-5 resulting from metal incorporation. It was found that 1.5% Zn content slightly increased aromatic compounds in contrast to 0.5%. Reaction temperature of 500 °C produced highest aromatics and lowest coke yield. It was proposed that the key to improved aromatic yield is hydrogen transfer activity.

Vichaphund et al. (2015) have investigated the influence of metal promoted HZSM-5 for pyrolysis of jatropha residues. HZSM-5 was promoted with Co, Ni, Mo, Ga and Pd using two methods i.e. ion exchange method and incipient wetness impregnation method. The study revealed that non-catalytic pyrolysis of jatropha residues engendered high amount oxygenated compounds, acids and nitrogen containing compounds. While addition of metal doped catalyst shifted product distribution toward aromatic compounds. Highest aromatic selectivity i.e. 97% was achieved by Mo-HZSM-5 at C/F of 10. Metal modified catalyst enhanced production of MAHs including benzene, toluene, xylene (BTX) with concurrent reduction in undesired PAHs. Wang et al. (2014) studied the conversion of pyrolytic vapors of Douglas fir sawdust pellets over Zn-ZSM-5 using varying loading of Zn (0, 0.5, 1, 2, 5 wt.%). 0.5 wt.% Zn-ZSM-5 produced highest aromatic hydrocarbon yield. It was noted that aromatic compounds were most abundant in bio-oil yield and their concentration increased with increase in packed bed temperature. All catalyst significantly decreased bio-oil yield and increased gas yield.

Table 2.7: Catalytic upgrading of different biomass over metal modified HZSM-5 catalysts

Ref.	Feedstock	Reactor Type	Mode	C/F	Metal doped on ZSM-5		Particle size mm	Type & heating rate °C/min	Temp. Pyr. Cat. °C	Flow rate ml/min	Findings
					Metal	wt. %					
Valle et al. (2010)	Pine	Fluidized-Bed Reactor	Ex-situ	-	Ni	1	0.8 - 2	-	450	-	Bio-oil conversion >90 % wt. with aromatics selectivity of 0.65
S. Zhang et al. (2018)	Rice husk	Fixed-Bed Reactor	Ex-situ	5	Fe	0.5, 1,2, 4,8	-	Fast	550 550	200	Optimum metal loading of Fe-ZSM-5 is 4 wt%. Increase in metal content decreased bio-oil yield.
Vichaphund et al. (2015)	Jatropha residues	Analytical Py-GC/MS	Ex-situ	1:1, 5:1, 10:1	Co, Ni, Mo, Ga, Pd	3	0.125	Fast -	500 -	-	Increased yield of MAH with concurrent decrease in PAH. 97% selectivity for Mo-ZSM5 at C/F =10
Sun et al. (2016)	Wood sawdust	Py-GC/MS	Ex-situ	10:1	Fe	15	-	Fast, 20 °C/ms	500-800 -	-	Fe-ZSM-5 increased selectivity toward MAH. Highest aromatics yield obtained at 600°C
Li et al. (2016)	Pine sawdust	Fixed-bed reactor	Ex-situ	0.5	Fe, Zr, Co	4	0.15–0.25	Fast	550 450-650	300	Zr-ZSM-5 promoted benzene and derivatives, Fe-ZSM-5 is selective towards naphthalene and derivatives, better performance than HZSM-5
Saraçoğlu et al. (2017)	Beech sawdust	Fixed-bed reactor	Ex-situ	0.1:1	Fe	1,5, 10	1.25-.85	500	500 -	400	Phenolic content increased from 29 to 50% with 10 wt% Fe-ZSM-5 compared to non-catalytic
Wang et al. (2014)	Douglas fir pellets	Packed-Bed Coupled with Microwave Pyrolysis	Ex-situ	2.2-7.8g/20	Zn	0.5, 1, 2	dia (5) length (20)	-	480 -	-	0.5 wt.% Zn-ZSM-5 produced highest aromatic hydrocarbon yield.
Fanchiang et al. (2012)	Furfural	Continuous Fixed Bed reactor	Ex-situ	-	Zn	0.5, 1.5	-	Fast	300-500 -	-	1.5% Zn yielded more aromatics than 0.5%. Temperature of 500 °C produced max. aromatics and lowest coke yield

Ref.	Feedstock	Reactor Type	Mode	C/F	Metal doped on ZSM-5		Particle size mm	Type & heating rate °C/min	Temp. Pyr. Cat. °C	Flow rate ml/min	Findings
					Metal	wt. %					
Veses et al. (2015)	Woody biomass	Auger reactor with Fixed-bed reactor	Ex-situ	-	Ni, Cu, Sn, Ga, Mg	1	-	Slow -	450 450	7	Increase production in hydrocarbons over Ni-ZSM-5 or Sn-ZSM-5
T.-L. Liu et al. (2017)	Shengli lignite	Drop tube reactor	In-situ	-	Co, Mo, Ni	5	-	Fast -	500 - 700	100	Ni-HZSM-5 proved most effective Metal promoted catalyst exhibited more deoxygenation activity
Mohammed et al. (2016)	Napier grass	Fixed-Bed Reactor	Insitu	0.5, 1,2,3	Zn	-	2.5	Slow 30	600	7000	Increase in catalyst loading decreased PAH formation. Zn-ZSM-5 increased selectivity of benzene
French et al. (2010)	Cellulose, lignin, and wood	Tubular Quartz Micro-Reactor With MBMS	In-situ	5–10	Ni, Co, Fe., Ga	-	-	Fast -	400	10000 (He), 10 (Ar)	Highest hydrocarbon yield was achieved by nickel substituted ZSM-5 i.e. 16 wt.%
Iliopoulou et al. (2012)	Beech wood	Circulating Fluid Bed Reactor	In-situ	0.5	Ni, Co	1-10	-	Fast -	500	100	Less dehydration activity and more selectivity for aromatics with both catalysts
Yaman et al. (2018)	Walnut shell	Fixed Bed Reactor	In-situ	0.33	Ni, Co	5	0.425-0.6	Fast -	500	100	Metal impregnated ZSM-5 yielded less water and favored formation of CO <sub>2</sub> over CO
Huang et al. (2012)	Rice husk, Sawdust, Sugarcane bagasse	Flowing fixed bed system	In-situ	0-1	La	6	<0.3	Fast -	600	-	Olefin yield for sugarcane bagasse > rice husk > sawdust > Olefin selectivity decreased with lignin content
Zheng et al. (2017)	Yunnan pine	Fixed-bed reactor	In-situ	2:01	Zn, Ni, Co, Ga, Cu, Mg	1,5, 10	0.25-0.42	250	500	150	Deoxygenation potential is as follows: Ga-ZSM-5 > Zn-ZSM-5 > Ni-ZSM-5 > Co-ZSM-5 > Mg-ZSM-5 > Cu-ZSM-5 > H-ZSM-5



### **2.7.2. Copyrolysis**

Copyrolysis is a method which employs two or more feedstocks. Copyrolysis has been realized as an effective method to augment bio-oil yield and quality without any modification in pyrolysis process. Essential feature of this method is the synergistic effects that is produced due to reaction of different feedstocks during pyrolysis. The bio-oil yield obtained during copyrolysis has a higher calorific value than that of biomass alone. Plastic and waste tires are most commonly used as cofeed in pyrolysis of biomass. Liquid yield derived from pyrolysis of plastic (or tires) alone cannot be directly mixed because of polar nature of bio-oil. Moreover, blending of these oil results in an unstable liquid that leads to phase separation after a short period of time. Therefore, copyrolysis has been found as a reliable technique to produce a liquid that is homogenous in nature. The pyrolysis of plastic waste is a promising Waste-to-Energy technology for production of liquid oil as a source of energy (Abnisa et al., 2014).

Plastic waste can be classified as industrial and municipal waste. Industrial plastic waste tends to be more homogenous whereas municipal plastics is heterogeneous in nature and more contaminated. Plastic waste is mainly comprised of high-density polyethylene (HDPE), low density polyethylene (LDPE), linear low-density polyethylene (LLDPE), polyethylene terephthalate (PET), polypropylene (PP) and polystyrene (PS). Most of waste plastic finds its way to landfills thus triggering environmental problems. Utilization of plastic in conjunction with biomass in pyrolysis process could have the added benefit of alleviating a waste disposal problem in addition to energy recovery. More waste plastic can be used as feedstock thus reduces the required landfill area, cost associated with waste treatment etc. In this regard, copyrolysis can be utilized as an alternative waste management strategy (Abnisa et al., 2014).

### **2.7.3. Catalytic co-pyrolysis**

Incorporation of hydrogen rich feedstock in catalytic pyrolysis of biomass could be helpful in mitigating problems such as high coke deposition over catalyst and low carbon yield. Waste plastics can be exploited as potential hydrogen donor as they are rich in

hydrogen. Massive quantities of plastic waste, generated each year present a cheap and abundant co-reactant to be incorporated in catalytic co-pyrolysis. Catalytic co-pyrolysis has been realized as a robust method to enhance aromatic production accompanied by coke reduction. Previous studies on catalytic co-pyrolysis have shown that positive synergistic effect between biomass and plastic increased the hydrocarbon content with concurrent decrease in solid residue. Increase in hydrocarbons is attributed to Diels–Alder reaction occurring between plastic derived olefins and biomass derived furans with subsequent dehydration reactions (Wang et al., 2014; Xue et al., 2016). (Dorado et al., 2015) suggested that the formation of a hydrocarbon pool favored the conversion of oxygenated compounds to aromatics.

Li et al. (2014) have evaluated the impact of different plastics (PS, LDPE, PP) addition in the catalytic pyrolysis of pine wood, lignin and cellulose. In this study, significant synergistic impact was observed for producing valuable hydrocarbons (aromatics) in cofeed of LDPE with cellulose/pinewood. It was suggested that oxygenates produced from thermal decomposition of cellulose reacted with LDPE derived olefins to form aromatic hydrocarbons. In addition to this, coke production was reduced considerably. For other combinations of plastic and biomass i.e PP/lignin, PS/lignin, PP/cellulose, PS/cellulose etc. synergistic impact was less pronounced.

Xue et al. (2016) co-pyrolyzed different biomasses (xylan, red oak, milled wood lignin, cellulose) with polyethylene in the presence and absence of ZSM-5. Main objective was to investigate interaction between biomass and PE during thermal decomposition followed by catalytic cracking of vapors. This study shown that incorporation of PE in pyrolysis of biomass reduced the production of bio-char and carbon-oxides. In addition to this, presence of biomass facilitated the depolymerization of polyethylene by enhancing yields of alkanes and olefins. Furthermore, augment in pyrolysis and catalytic temperature in copyrolysis of red oak and PE favored the production of aromatic hydrocarbons and reduced the catalytic coke.

Table 2.8: Use of HZSM-5 catalyst in conjunction with different plastics for upgrading

Ref.	Feedstock		Catalyst	Biomass /Plastic	Reactor Type	Mode	C/F	Type & heating rate	Temp. Pyr. Cat.	Findings
	Biomass	Plastic						°C/min	°C	
<b>Lin et al. (2017)</b>	Wood powder	HDPE, PP	HZSM-5 (25,50,60)	1:1	Py-GC/MS	In-situ	1:1	Fast 20 °C/ms	550	Optimum yield of aromatics from wood powder and PP/HDPE composite over HZSM-5 with SAR of 25
<b>Duan et al. (2017)</b>	Lignin	PP	ZSM-5	1:0, 1:1, 1:2, 2:1, 0:1	Microwave assisted pyrolysis	Ex-situ	0,0.2 5, 0.5, 1	Fast	550 200-350	Minimum value of 6.74% for oxygenates with lignin/PP =1:1. Optimum catalytic temp is found to be 250 °C for bio-oil yield
<b>Mullen et al. (2017)</b>	Switch-grass	PE	HZSM-5	1:1	Py-GC/MS	Ex-situ	2:1 & 4:1	Fast	650 500	Addition of PE to biomass is beneficial to reducing coke formation. However, effect of catalyst deactivation diminished at F/C=4:1
<b>Kim et al. (2017)</b>	Yellow Poplar, Torrefied Yellow Poplar	HDPE	HZSM-5 , Al-MCM-41	1:1	tandem micro-pyrolyzer	In-situ & Ex-situ	10:1	Fast	600	Insitu catalytic co-pyrolysis produced more aromatics compared to insitu. HZSM-5 elucidated better activity for aromatics production
<b>Rezaei et al. (2017)</b>	Yellow poplar	HDPE	meso MFI, meso Y , Al-SBA-15	0, 0.25, 0.5, 0.75, 1	TMR-GC/MS	In-situ	10:1	Fast	600	meso MFI showed highest selectivity for aromatics production. Synergistic effect was observed during co-pyrolysis.
<b>H. Zhang et al. (2018)</b>	Sugarcane bagasse	Bio-plastic	USY, HZSM-5	1:1, 1:2, 1:3, 1:4.	Py-GC/MS	Ex-situ	20,16 , 8, 6, 4,2	Fast	400-700	Optimum F/C ratio: 1:6 & 1:16 for HZSM-5 and USY. Aromatics selectivity is increased by

Ref.	Feedstock		Catalyst	Biomass /Plastic	Reactor Type	Mode	C/F	Type & heating rate	Temp. Pyr. Cat.	Findings
	Biomass	Plastic						°C/min	°C	
										10 times by raising temperature from 400 -700 °C
<b>Y. Wang et al. (2017)</b>	Waste vegetable oil	HDPE	ZrO <sub>2</sub> (75.8%) Al <sub>2</sub> O <sub>3</sub> (8.4%) TiO <sub>2</sub> (4.2%)	3:1,1:1,1:3	Autoclave	In-situ	0,0.0 5,0.1, 0.2	Slow 10	340-460	Maximum oil yield of 63 wt.% obtained at 430 °C maximum alkanes content (97.85 wt.%) obtained at optimal conditions.
<b>Li et al. (2013)</b>	Cellulose	LDPE	ZSM-5	1:1	Pyro probe pyrolyzer	In-situ	10:1	Fast 20 °C/ms	650	Positive synergistic effect in aromatics yield (47.46%) was observed with decreased rate of coke deposition
<b>Zhang et al. (2015)</b>	Corn stalk	HDPE	HZSM-5	4:1, 3:1 2:1, 1:1 ,1:2 1:3 ,1:4	Py-GC/MS	Ex-situ	2:1	Fast 20 °C/ms	550-800	Maximum aromatics were achieved at the temperature of 550 °C, however, 700 °C temperature gave max. hydrocarbon yield.
<b>Xue et al. (2016)</b>	Cellulose, xylan, red oak, wood lignin	PE	HZSM-5	1:1	Tandem micro-pyrolyzer	Ex-situ	20:1	Fast -	400-700	Augment in pyrolysis and catalytic temperature in copyrolysis of red oak and PE favored the production of aromatic hydrocarbons and reduced the catalytic coke
<b>Zhang et al. (2014)</b>	Pine sawdust	PE, PP, PS	Spent FCC, $\gamma$ Al <sub>2</sub> O <sub>3</sub> LOSA-1	1:4-4:1	Fluidized-bed reactor	Ex-situ	-	Fast -	400-650	LOSA-1 have shown a better catalytic activity compared to $\gamma$ Al <sub>2</sub> O <sub>3</sub> and spent FCC

## Chapter 3 MATERIALS AND METHODS

This chapter provides information on feedstock preparation, catalyst synthesis, and pyrolysis system used in this study. It details out the technique used for fractionation of the upgraded bio-oil. It also explains the analytical procedures adopted for the characterization of materials and products.

### 3.1 Feedstock preparation

Wheat straw, as a widespread agricultural residue, investigated in the study was collected from a local farm. It was pre-dried in sunlight for one day to decrease moisture content. It was shredded, comminuted and sieved mechanically to obtain a particle size of less than 0.8mm. Wheat straw was dried in oven overnight at 105 °C to remove physisorbed moisture prior to pyrolysis. Polystyrene (PS) (beads of average size 1mm) was purchased commercially from local market and used without any modification.



Figure 3.1: Feedstock preparation (a) Raw form (b) Shredded form (c) Grinded form

Feed stocks were characterized by proximate, elemental and compositional analysis as per standard methods mentioned in Table 4.1. Elemental analysis was performed on SDCHN435 (SUNDY) elemental analyzer to determine C, H, N and O content. Gross calorific values were determined by 6200 Isoperibol Calorimeter. Thermal degradation behavior of feed materials was evaluated using a thermo gravimetric analyzer (Mettler Toledo) under nitrogen atmosphere. The flow rate of purge gas was maintained at

20ml/min. The sample was placed in crucible and heated from the ambient temperature up to 620 °C with a heating rate of 10 °C min<sup>-1</sup>. The thermal decomposition of WS and PS was carried out separately.

### 3.2 Catalyst preparation

In this study, parent Zeolite ZSM-5 with SiO<sub>2</sub>/Al<sub>2</sub>O<sub>3</sub> molar ratio of 38 was purchased commercially in NH<sub>4</sub><sup>+</sup> form. Prior to modification ZSM-5 was calcined in muffle furnace at 550°C for 4h to convert it into protonic form i.e. HZSM-5. HZSM-5 support was further promoted with four transition metals (Fe, Ni, Co, Zn) through incipient wetness impregnation method. Nitric salts, nickel nitrate hexahydrate [Ni (NO<sub>3</sub>)<sub>2</sub>·6H<sub>2</sub>O], zinc nitrate hexahydrate [Zn (NO<sub>3</sub>)<sub>2</sub>·6H<sub>2</sub>O], cobalt nitrate hexahydrate [Co (NO<sub>3</sub>)<sub>2</sub>·6H<sub>2</sub>O], ferric nitrate nonahydrate [Fe (NO<sub>3</sub>)<sub>3</sub>·9H<sub>2</sub>O] were used as the metal precursors. These salts were purchased from Dae-Jung Chemicals and used without further purification.

In order to obtain a suitable particle size with adequate mechanical stability and attrition resistance, bentonite was added as a binder. HZSM-5 was mixed with bentonite in 70/30 (w/w) ratio. The stoichiometric quantities of metal salts were dissolved in deionized water followed by addition of HZSM-5 and bentonite mixture. Each catalyst was based on 5% metal content. For 100g of parent HZSM-5, the required amount of Zn (NO<sub>3</sub>)<sub>2</sub>·6H<sub>2</sub>O, Ni (NO<sub>3</sub>)<sub>2</sub>·6H<sub>2</sub>O, Fe (NO<sub>3</sub>)<sub>3</sub>·9H<sub>2</sub>O and Co (NO<sub>3</sub>)<sub>2</sub>·6H<sub>2</sub>O is 22.7g, 24.8g, 36.1g, 24.7g respectively. The suspension was stirred at 300 rpm for 4 h on magnetic stirrer hot plate to attain dispersion of metal ions on catalyst support. Here agglomeration and impregnation were carried out simultaneously.

The prepared slurry was then dried at 105 °C for 24h. After that, deionized water as an adhesive was added in catalyst powder to make a paste which was then molded to rods through a hand extruder. The extruded rods were dried in air, cut and sieved to obtain pellets with particle size in the range of 0.8-2mm. Thereafter, catalysts were re-calcined for 4 h at 500 °C/min to 550 °C in static air which implies that each metal is dispersed on external and internal surface of catalyst as corresponding metal oxide. The post-treated zeolites were denoted as M-ZSM-5, where M represents loaded metal oxide. All

synthesized catalysts were kept in desiccator before experiment to avoid water adsorption.



Figure 3.2: Catalyst preparation (a) Parent HZSM-5 (b) Paste formation (c) Extrusion (d) Fe-ZSM-5 (e) Zn-ZSM-5 (f) Co-ZSM-5

### 3.3 Pyrolysis Setup & Operation

A sequential two-stage catalytic pyrolysis setup consisted of batch-type two tubular fixed bed reactors. The reactors were constructed of stainless-steel (SS-316) because it can withstand high temperature. Moreover, corrosive nature of pyrolysis vapors necessitates the use of a corrosion resistant reactor's material. First reactor (R1) was used for pyrolysis, with dimensions of 500 mm length and an inner diameter of 108 mm while second reactor (R2) was used as catalytic cracker having dimensions of 360mm length and 42mm inner diameter. Both reactors were arranged in vertical position, connected through a 1/4" stainless steel tube having length of 3". This tube was insulated with ceramic wool to avoid heat loss which may result in inline condensation. Reactors were equipped with connections for inert gas entry and products output.

Cylindrical ceramic heating elements, wrapped around reactors, were used to provide heat externally. A k-type thermocouple as sensor was installed vertically at the middle of each reactor to monitor temperature inside. The temperature of both electrically heated reactors was controlled independently by PID controllers. Both heater and reactor tube surrounded by ceramic wool for the purpose of insulation. Nitrogen gas was used as carrier gas and to provide inert atmosphere. Gas flow rate was controlled by rotameter mounted at upstream side of pyrolysis reactor. N<sub>2</sub> gas was introduced from bottom of pyrolysis reactor. A stainless-steel mesh (#100) supporting ceramic wool, was fixed at center of catalytic reactor onto which the catalyst was loaded. Ceramic wool was used to filter unreacted char entering in catalyst layer. A water-cooled heat exchanger was designed to entrap condensable vapors. Temperature of condenser was kept at -5°C by using salty ice. The schematic diagram of experimental setup is shown in Fig 3.3.

Each experiment was carried out under atmospheric pressure. In each catalytic run, 100 grams of dried feedstock was loaded onto sample position in first reactor and 50 grams of activated catalyst was placed as fixed bed in second reactor. Reactors were closed tightly to avoid any leakage during experimental run. Prior to experiment, the whole system was flushed with 300 ml/min of nitrogen gas for 30 minutes to create an inert atmosphere inside. During sweeping, a soap bubble test was performed to ensure air tightness. After that, catalytic reactor was pre-heated to desired temperature. Subsequently, temperature of pyrolysis reactor was raised up-to predetermined temperature with a heating rate of 35 °C/min. and held for approximately 30mins or until no more release of vapors was observed, in order to ensure complete evolution of pyrolytic vapors.

During the experiment, N<sub>2</sub> flow rate was maintained at 100ml/min. Volatile phase evolved during pyrolysis of feedstock was driven through catalyst bed. Upgraded vapors were then passed through ice-water condenser and condensable pyrolytic vapors were collected in a glass receiver. Non-condensable gases escaped at the end of cooling traps. After the reaction was completed, system components were dismantled and reactors were cooled to ambient temperature using fan. A constant flow of nitrogen gas was



maintained during cooling to avert bio-char oxidation. Subsequently, bio-char and spent catalyst were recovered from reactors. The yields of bio-char, bio-oil and deposited coke on catalyst were calculated gravimetrically. Bio-oil samples were kept in refrigerator prior to analysis. Experimental runs were conducted in duplicate to ensure reproducibility

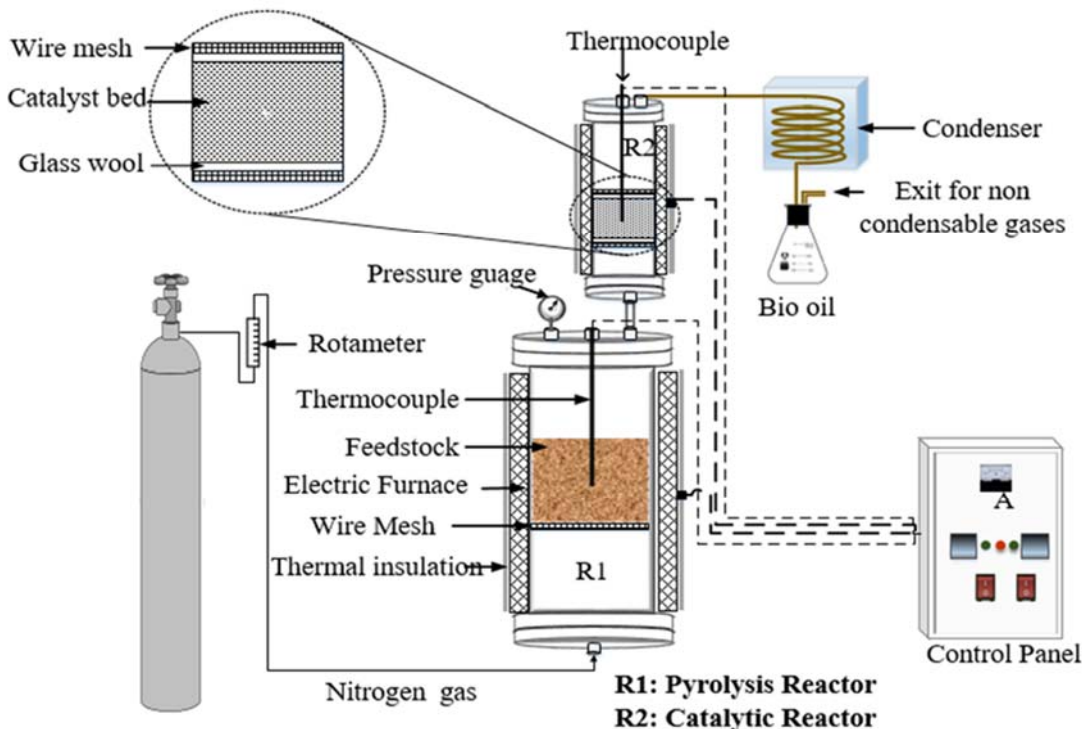


Figure 3.3: The schematic diagram of experimental setup

### 3.4 Experimental design

Experimental runs were conducted in two phases. In phase 1, optimum pyrolysis temperature was investigated to maximize liquid product yield for catalytic experiments. For this, WS to PS ratio was taken as constant i.e. 1:1 and copyrolysis was carried out at four different temperatures i.e. 500 °C, 550 °C, 600 °C, 650 °C. Catalytic reactor was maintained at 500 °C and kept empty. Pyrolysis temperature that gave optimum yield was then selected for further catalytic runs.

In phase 2, feedstock to catalyst ratio was fixed as 2:1. HZSM-5 and all 4 M-ZSM-5 catalysts were then tested for pyrolysis products' yield and bio-oil quality.

Phase 1	WS:PS = 1:1 No catalyst	Pyrolysis temperature				
		500 °C	550 °C	600 °C	650 °C	
Phase 2	WS:PS = 1:1 F: C = 2:1	Catalyst type				
		HZSM-5	Zn-ZSM-5	Co-ZSM-5	Ni-ZSM-5	Fe-ZSM-5

\* C= Catalyst, F=Feedstock

### 3.5 Oil separation

Liquid product formed two distinct phases due to density difference; lower aqueous and upper organic phase. These two phases were separated using a separating funnel with 4 hours retention time. Organic phase was then passed through bed of anhydrous sodium sulphate to remove any moisture present. Thereafter, organic phase was used for subsequent analysis.

### 3.6 Catalyst characterization

HZSM-5 and all four metal modified catalysts were characterized by number of analytical techniques to evaluate the effect of metal addition on physiochemical properties of catalysts. Following section describes experimental procedure with some theoretical background for each technique.

#### 3.6.1 N<sub>2</sub> physisorption

Textural properties of metal impregnated catalyst were measured using a surface area analyzer (Gemini VII 2390, Micromeritics). Prior to analysis, samples were out-gassed in a flowing N<sub>2</sub> gas at 300°C for 8h. Adsorption-desorption isotherms were measured at 77K using liquid N<sub>2</sub> as an adsorbate at a relative pressure ranging from 0.1-0.9. Specific surface area of catalyst was determined by multipoint BET (Brunauer-Emmett-Teller) theory using linear portion of BET plot. T-plot method was employed to calculate

micropore volume. Measurement of pore size distribution was carried out using BJH (Barrett-Joyner-Halenda) method. Total pore volume was calculated at a relative pressure  $P/P_0 = 0.99$

### **3.6.2 Powder X-ray diffraction (XRD) spectroscopy**

Powder X-ray diffraction (XRD) is a non-destructive analytical technique used to characterize crystalline solid materials. Bragg's law is used to determine interference pattern of X-ray radiations scattered by crystals

$$n\lambda = 2d\sin\theta$$

The crystal properties of HZSM-5 and MZSM-5 were determined by using diffractometer employing Cu-K $\alpha$  radiation, at an operating voltage of 40 kV and current of 30 mA. XRD patterns were recorded at a continuous scanning in the angular range of 10–70° ( $2\theta$ ) with a step size of 0.02. PANalytical X'Pert High Score Plus software was employed to carry out phase identification. The degree of crystallinity was determined on the basis of characteristic peak's intensity at  $2\theta = 7-9$  and  $22-25^\circ$ .

### **3.6.3 SEM-EDS**

The microstructure of HZSM-5 and MZSM-5 catalyst was characterized by scanning electron microscopy (TESCAN VEGA3) coupled with energy dispersive spectroscopy (51-ADD0007, Oxford Instruments). The acceleration voltage was set as 20kV for analysis. SEM was used to image catalyst morphology while elemental analysis was carried out using EDS.

## **3.7 Liquid product analysis**

### **3.7.1. GC-MS**

The organic phase of pyrolysis oil was analyzed by GCMS using Shimadzu QP2010 Ultra gas chromatograph. A capillary column DB-5MS (30 m  $\times$  0.25 mm ID  $\times$  0.25  $\mu$ m) was used in system. Oven temperature was programmed from 30°C (1 min hold) to 290 °C with a heating rate of 8 °C/min and held for 2min. The injector temperature, interface

temperature, split ratio are 285 °C, 295°C and 1:80 respectively. Helium was used as carrier gas with a constant flow rate of 20ml/min. The MS was operated in EI mode at 70 eV and the ion source temperature was set at 230 °C. National Institute of Standards and Technology (NIST 11) mass spectral library was employed to identify peaks of chromatograms. Integrated peak area values of chromatograms were utilized for quantitative determination of chemical compounds

### **3.7.2. Physical properties**

Organic liquid product was also analyzed for its main fuel properties, respective standards methods of which are mentioned in table 4.4. Redwood viscometer was used to measure kinematic viscosity of oil samples at 40 °C . Flash, fire and pour points were measured by their corresponding analyzers (Koehler Instrument company INC.) Gross calorific values were determined by 6200 Isoperibol Calorimeter.

## Chapter 4 RESULTS AND DISCUSSION

### 4.1 Feedstock analysis

#### 4.1.1. Physicochemical characteristics of feedstocks

The results for proximate, ultimate and compositional analysis for the feedstocks are presented in Table 4.1. Volatile matter in the feedstock corresponds to the expected liquid yield in pyrolysis. Higher the volatile matter, more is the potential of liquid yield. On the other hand, high ash content decreases the liquid yield and contributes to formation of solid residue after pyrolysis (Farooq et al., 2018b). The result for proximate analysis revealed that PS was solely composed of volatile matter while WS contained 68.3% volatile matter. Therefore, it is expected that PS will contribute more to liquid yield as compared to WS.

Table 4.1: Physico-chemical characteristics of selected feedstocks

<b>Feedstock</b>	<b>Test method</b>	<b>Wheat Straw</b>	<b>Polystyrene</b>
Dry density (g/cc)	ASTM D 1895B	0.151	0.61
Heating value (MJ kg <sup>-1</sup> )	ASTM D 5865	17.19	42
<b><i>Proximate analysis (wt.%)</i></b>			
Moisture content	ASTM D 3173	9	-
Ash	ASTM D 3174		-
Volatile matter	ASTM D 3175		99.9
Fixed carbon	By difference		0.1
<b><i>Ultimate analysis (wt.%)</i></b>			
C	ASTM D 5373-02	47.74	90.4
H	ASTM D5373-02	5.5	8.6
N	ASTM D5373-02	0.7	0.4
O	By difference	46.06	0.6
H/C <sub>eff</sub> <sup>a</sup>	-	<0	1.1
<b><i>Biochemical analysis (wt.%)</i></b>			
Cellulose	ASTM D1103	32.5	-
Hemicellulose	ASTM D1104	38.3	-
lignin	ASTM D1105	20.7	-
Extractives <sup>b</sup>	-	8.5	-

<sup>a</sup> H/C<sub>eff</sub> = (H-2O)/C

<sup>b</sup> Extraction with acetone

The ultimate analysis displayed comparatively higher content of hydrogen and very low oxygen content in PS in contrast to WS due to which the H/C<sub>eff</sub> ratio of PS (1.1) was found to be much higher than that of WS (-0.06). H/C<sub>eff</sub> ratio indicates the relative content of hydrogen in feedstock (Zhang et al., 2015). Higher H/C<sub>eff</sub> shows that PS is hydrogen-rich and could be added as the hydrogen donor during the catalytic copolyolysis. Biochemical analysis displayed that almost 70% of WS was composed of cellulose & hemicellulose which is easily decomposed. Owing to higher oxygen content (46.1% against 0.6% of PS), the HHV of WS (17.2 MJ/kg) was found to be much lesser than that of PS (42 MJ/kg). Also, the density of PS was higher as compared to WS.

#### **4.1.2. Thermal degradation of feedstocks**

The TGA technique was used to evaluate the thermal degradation characteristics of the feedstocks at a heating rate of 20 °C/min. Thermal degradation profiles of WS and PS are depicted in the Fig. 2. The TGA curve of WS revealed a 3-stage decomposition profile. There was no mass loss till 107 °C and initial mass loss was observed in the temperature range of 100-250 °C resulting in 3% degradation of initial sample. This stage corresponds to the removal of physisorbed water content accompanied by hydrolysis of extractives (Ghorbannezhad et al., 2018; Shah et al., 2019).

Devolatilization phase of WS commenced at about 250 °C and continued up to 400 °C with maximum mass loss of about 58%. According to previously reported data (Ahmed et al., 2018), this stage is associated with the progressive decomposition of cellulose and hemicellulose content. After 400 °C, no significant weight loss was witnessed and could be related to very slow decomposition of highly stable lignin (Ghorbannezhad et al., 2018). On the other hand, the TGA curve of PS depicted an insignificant mass loss up to 360 °C. However, a distinct weight loss step was visualized at temperature ranging from 365-500 °C and accounted for prominent mass loss of 92%. Thereafter, mass of PS became relatively constant up to the final temperature. Wu et al.(2014) reported similar thermal profile for PS.

It should be noted that, both feedstocks exhibited completely different degradation patterns. WS decomposition started at lower temperature in contrast to PS which is likely due to inherent structural difference, as WS is composed of lignin, moisture and holocellulose whereas PS is an aromatic polymer (Dewangan et al., 2016). Moreover, negligible amount of solid residue was noticed for PS at the final temperature of TG measurement, indicating almost complete vaporization.

While, higher residual content of about 29% in case of WS could be ascribed to higher percentage of fixed carbon and ash in biomass sample (Brebou et al., 2010). This is also evident from proximate analysis of WS mentioned in the Table 4.1. From TGA analysis, it can be concluded that substantial mass loss for both feedstocks took place till 500 °C and it is anticipated that main pyrolysis reactions occurred between 250-500 °C. These results are in good agreement with previously reported TGA literature (Elsayed et al., 2016; Farooq et al., 2018a).

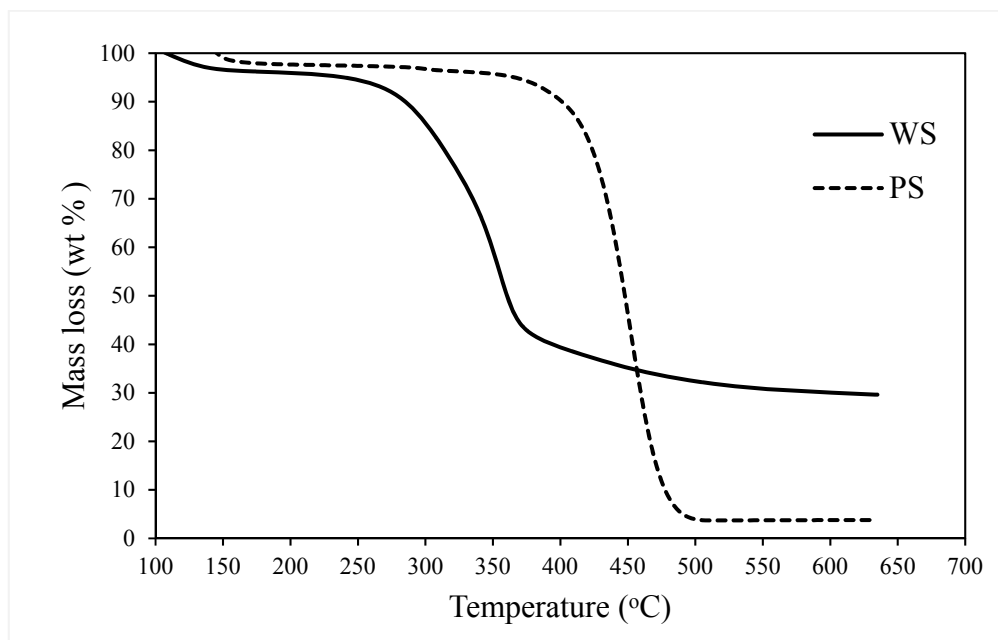


Figure 4.1: TGA plot of WS and PS

## 4.2 Catalyst Characterization

### 4.2.1 XRD results

XRD patterns of HZSM-5 and transition metal loaded MZSM-5 are shown in figure 4.2. Main peaks of HZSM-5 were occurred at  $2\theta$  22-25° with an orthorhombic form. All the metal modified catalysts exhibited similar characteristic peaks in the range of 7-9° and 23-25° as HZSM-5. This indicate that crystalline structure of HZSM-5 support remained intact by metal addition. No distinct characteristic response corresponding to metal oxides was detected. It elucidates that all four metals (Fe, Ni, Co, Zn) in the form of their respective oxides were homogenously dispersed on the surface of metal impregnated catalysts. However, peak intensity for Zn-ZSM-5 was slightly lower than parent HZSM-5 which could be attributed to metal addition onto support.

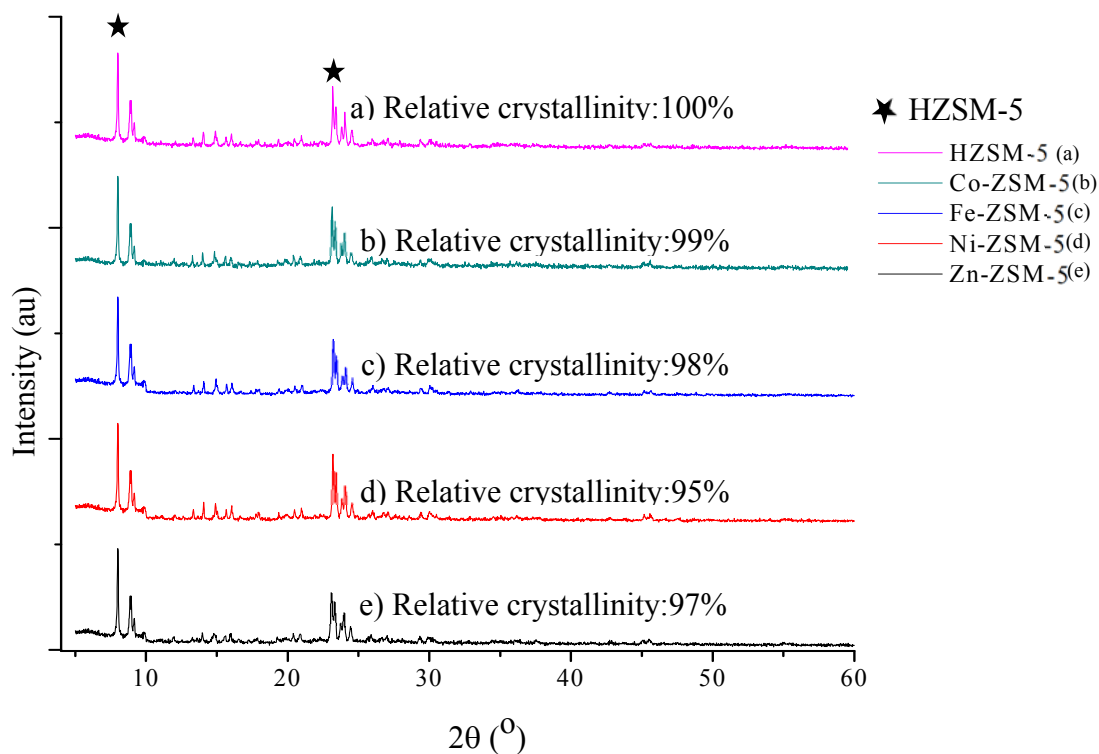


Figure 4.2: XRD patterns of parent and metal based catalysts



## 4.2.2 SEM analysis

SEM images revealed a smooth surface for parent HZSM-5 catalyst. While in the case of synthesized catalysts, metal oxides appeared as agglomerates due to the interconnection between the respective metal oxide and HZSM-5 particles, which suggests successful dispersion of metals ions on the surface of support. Moreover, metal impregnated catalysts exhibited no apparent change in the surface morphology of particles, indicating that zeolite HZSM-5 retained its microstructure after impregnation. SEM micrographs of HZSM-5 and MZSM-5 catalysts are shown in figure 4.3.

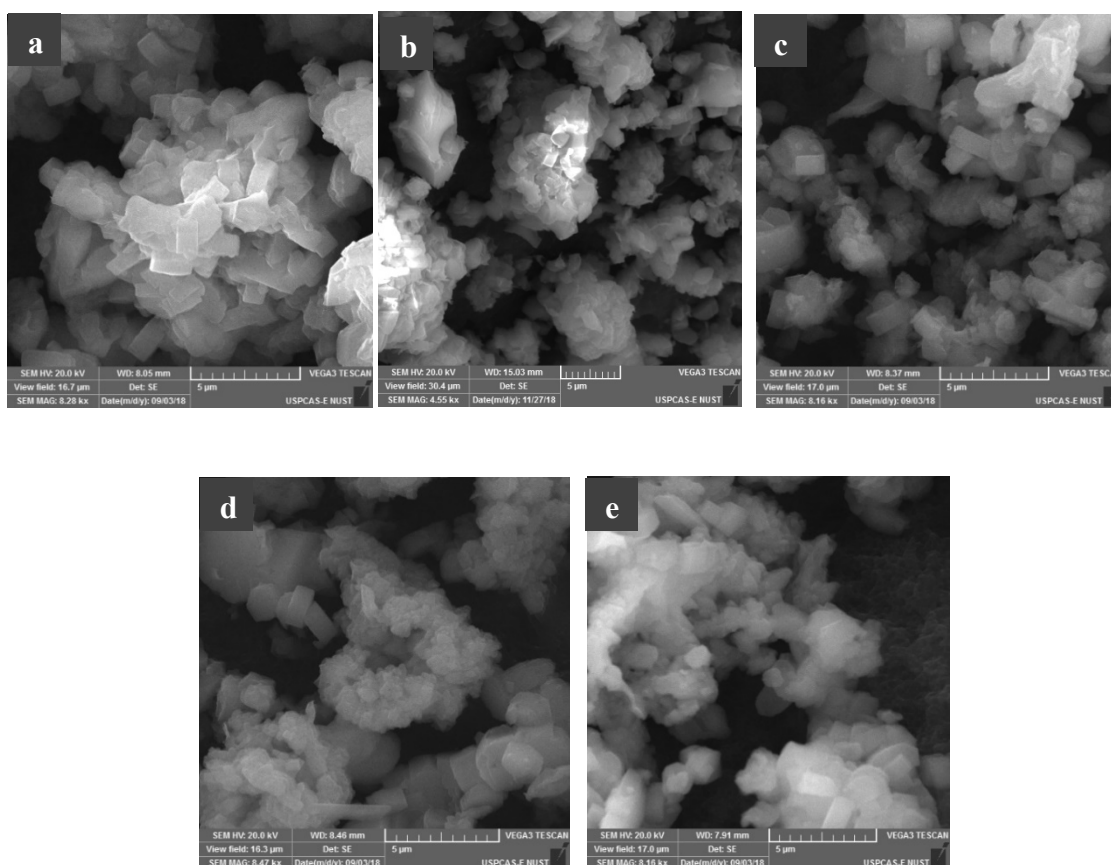


Figure 4.3: SEM images of (a) Parent HZSM-5 (b) Fe-ZSM-5 (c) Co-ZSM-5 (d) Ni-ZSM-5 (e) Zn-ZSM-5

### 4.2.3 EDS analysis

Metal content on catalyst support was calculated from average of at least three different points. Actual metal loading on impregnated catalyst was lower as compared to nominal loading i.e. 5%. This difference is expected and may be attributed to loss to of salt solution in lab equipment being used during impregnation.

Table 4.2: Metal content in modified catalysts

Samples	Nominal metal loading wt %	Actual metal loading wt %
HZSM-5	-	-
Co-ZSM-5	5	2.96
Ni-ZSM-5	5	3.73
Fe-ZSM-5	5	3.99
Zn-ZSM-5	5	3.37

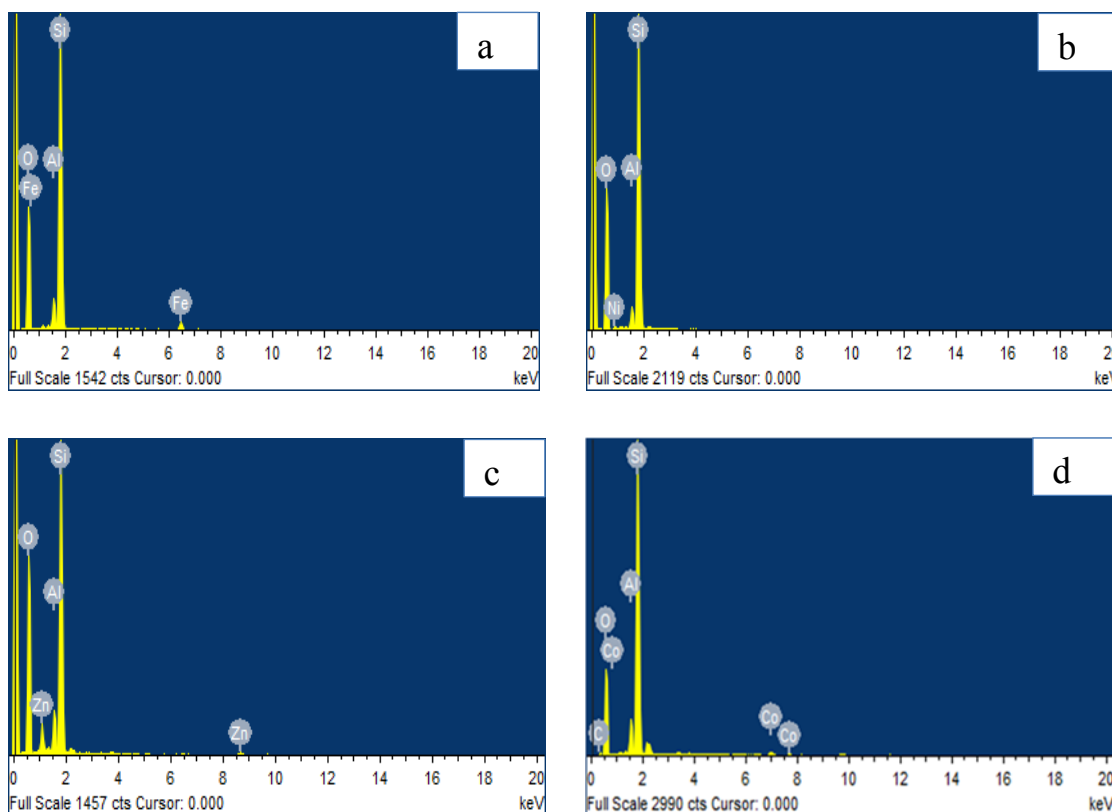


Figure 4.4: EDS analysis of (a) Fe-ZSM-5 (b) Ni-ZSM-5 (c) Zn-ZSM-5 (d) Co-ZSM-5

#### 4.2.4 Textural properties of catalyst

The textural properties such as total pore volume, micropore & mesopore volume, specific surface area, and pore size of the parent and modified HZSM-5 catalysts are summarized in Table 4.3. These properties are known to have a considerable effect on catalyst performance and thus the reaction mechanisms during catalytic pyrolysis (Balasundram et al., 2018).

Adsorption isotherms obtained for each sample resemble type IV isotherm according to the classification by the IUPAC. The result showed that parent HZSM-5 exhibited the highest  $S_{BET}$  (210  $m^2/g$ ), and that the addition of metals to catalyst resulted in the reduction of  $S_{BET}$ . Among all four MZSM-5 catalysts, Fe-ZSM-5 had the least reduction in  $S_{BET}$ . Similarly,  $V_{total}$ ,  $V_{meso}$ , and  $V_{micro}$  were also found to be reduced by impregnation. It might be attributed to the presence of active metal oxide aggregates on the external surface or deposition into the pores of HZSM-5, as confirmed by SEM analysis (Zheng et al., 2017). However, no significant change in pore size was observed after impregnation.

Table 4.3: Porosity characteristics of parent and metal based catalysts

	$S_{BET}$ ( $m^2/g$ )	$V_{total}$ ( $cc/g$ )	$V_{meso}$ ( $cc/g$ )	$V_{micro}$ ( $cc/g$ )	Pore size ( $nm$ )
HZSM-5	210	0.224	0.14	0.084	4.88
Zn-ZSM-5	199	0.138	0.055	0.083	4.75
Co-ZSM-5	194	0.142	0.062	0.080	4.5
Ni-ZSM-5	196	0.149	0.076	0.073	4.67
Fe-ZSM-5	206	0.152	0.077	0.075	4.76

#### 4.3. Product analysis

##### 4.3.1. Effect of temperature on product yield

The first set of pyrolysis runs was conducted between 500 and 650 °C with interval of 50 °C in order to appraise the influence of varying temperature on product distribution from PS/WS non-catalytic co-pyrolysis. The ratio of WS to PS was taken as 1:1.

Copyrolysis was conducted in pyrolysis reactor and pyrolyzates were then driven through vacant/empty catalytic reactor that was maintained at 500 °C. The yields of solid residue, liquid oil and gas products are presented in figure 4.5.

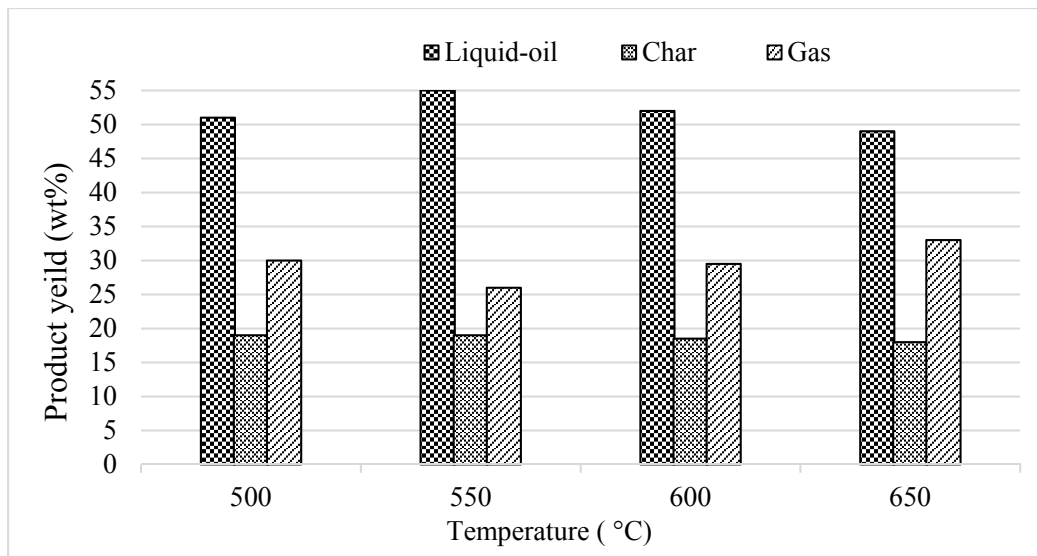


Figure 4.5: Products' distribution at varying temperatures

It can be seen that, with augment in pyrolysis temperature, liquid yield was increased from 51% at 500 °C to 55% at 550 °C as increased temperature facilitated more vapor release (Ro et al., 2018). Thereafter, liquid yield tapered down to 49% by further enhancing temperature from 550 to 650 °C with concurrent rise in gas yield. This can be attributed to further breakdown of pyrolysis intermediates to lighter hydrocarbons at higher temperatures (Fu et al., 2018). Among the four temperatures tested in this study, the liquid yield passed through a maximum at 550 °C. Hence, pyrolysis temperature of 550 °C was selected in order to elucidate the performance of catalyst (Fu et al., 2018). However, the yield of solid residue did not vary significantly.

#### 4.3.2. Effect of metal loaded catalysts on product yield

The influence of HZSM-5 and metal loaded catalysts on products distribution in comparison with non-catalytic experiment is presented in figure 4.6. Organic liquid yield here is referred to as organic fraction after removing aqueous phase i.e. Water. Pyrolysis was carried out at 550 °C which was proved to be optimum temperature for

co-feed of WS and PS at 1:1. However, the temperature of catalytic reactor was maintained at 500 °C. Non-catalytic run was conducted under the similar operating conditions in the absence of catalyst bed.

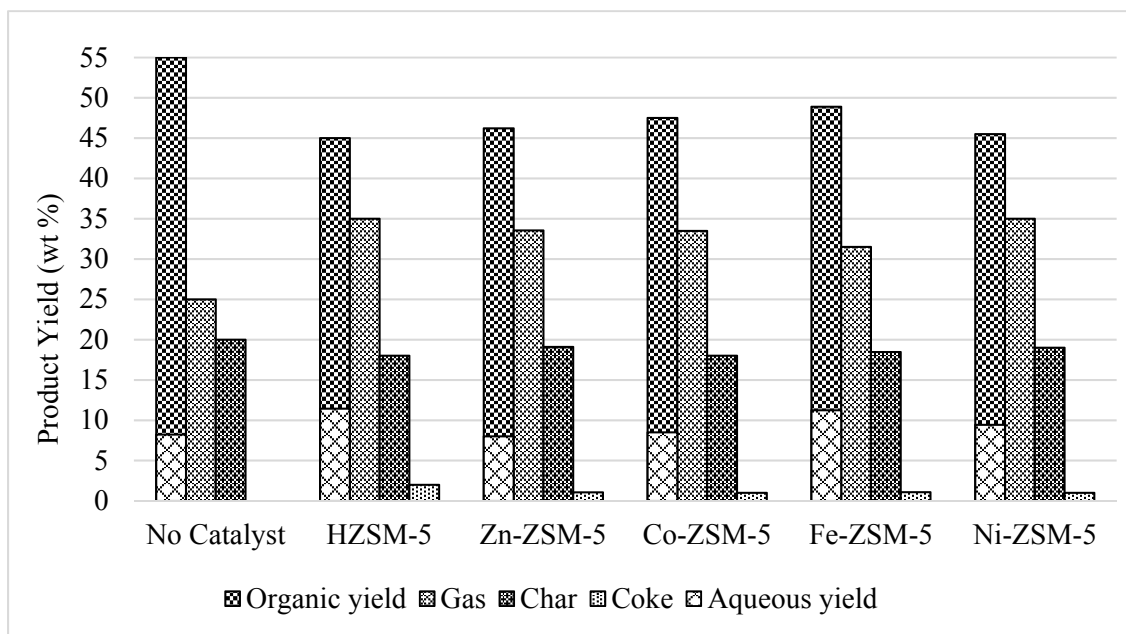


Figure 4.6: Pyrolytic products obtained with and without catalysts

Moreover, the untainted HZSM-5 catalyst was employed in order to evaluate and compare the effect of metal incorporation in HZSM-5. As it can be seen, addition of HZSM-5 substantially reduced the total liquid yield, from 55% down to 45%, while simultaneously increased the formation of solid and gas products in comparison to non-catalytic experiment. This could be explained by the fact that, in the presence of catalyst, pyrolyzates undergo a suite of cracking, dehydration, decarbonylation and decarboxylation reactions resulting in severe cracking of volatiles toward non-condensable gases (Yaman et al., 2018). In addition to this, catalytic pyrolytic oil contained more water content (11.4%) in contrast to non-catalytic (8.2%) thus reducing organic product yield. Higher amount of water content may be attributed to pronounced decarboxylation/dehydration reactions occurring on acids sites of HZSM-5 (Hu et al., 2017; Ren et al., 2018). However, impregnation of parent HZSM-5 with metals resulted in relatively higher organic liquid yield compared to unmodified one. Co-ZSM-5

produced maximum organic liquid yield (39%) followed by Zn-ZSM-5 (38.2%), Fe-ZSM-5 (37.7%) and Ni-ZSM-5 (36.1%). Besides, lesser water formation was observed for all metal substituted catalysts. This indicates that presence of added metal sites facilitated the decarboxylation and decarbonylation reactions while inhibiting dehydration reactions (Yaman et al., 2018).

One of the major drawbacks associated with thermo-catalytic upgrading over HZSM-5 is coke deposition over catalyst. Polymerized and dehydrated/ dehydrogenated compounds from pyrolytic vapors are responsible for coke formation resulting in rapid catalyst deactivation (Veses et al., 2015). In this study, the coke yield was reduced by approximately 50% over metal promoted catalysts as compared to parent HZSM-5. This might be related to mild acidic strength of metal doped catalyst. Hence it is worth mentioning that incorporation of metal is helpful in attenuating rate of coke formation. However, the char yield of around 19 wt.% was hardly affected in all catalytic experiments because the catalyst was applied in a separate reactor which catalyzed only pyrolyzates without effecting pyrolysis reaction.

#### **4.3.3. Chemical properties of OP**

The OP samples obtained in the presence and absence of catalysts were characterized by GC-MS for chemical composition analysis. The relative content of each component is expressed in term of percent peak area of chromatogram. The identified chemical compounds were further categorized into three main groups i.e. MAHs, PAHs and oxygenated compounds (OCs). MAHs encompass mainly BTEX (benzene, toluene, ethyl-benzene, and xylene), styrene, and other lighter monoaromatics. Whereas, PAHs include indene, naphthalene, and derivatives predominantly. OCs primarily comprise of oxygen-containing functionalities such as ketones, aldehydes, acids, alcohols, and ethers. Fig. 7 shows the component distribution profile for non-catalytic, HZSM-5 and its impregnated catalyst versions i.e. Co-ZSM-5, Zn-ZSM-5, Fe-ZSM-5, and Ni-ZSM-5. As can be seen in graph, non-catalytic copyrolysis engendered aromatic hydrocarbons dominantly, relative content of which measured up to 81.1%. This is strongly related to inherent aromatic nature of PS. As other authors have reported, PS upon thermal

degradation, cracks to styrene monomer (predominately) and other lighter aromatics through simple depolymerization (Sanahuja-Parejo et al., 2018). Consequently, styrene and derivatives (41.1%) were the major products obtained from PS/WS thermal pyrolysis. The relative abundance of other aromatics including BTEX, other MAHs and PAHs was 26.1%, 8.4%,5.5% respectively. However, significant amount (19%) of undesirable OCs was also observed which were possibly derived from the biomass.

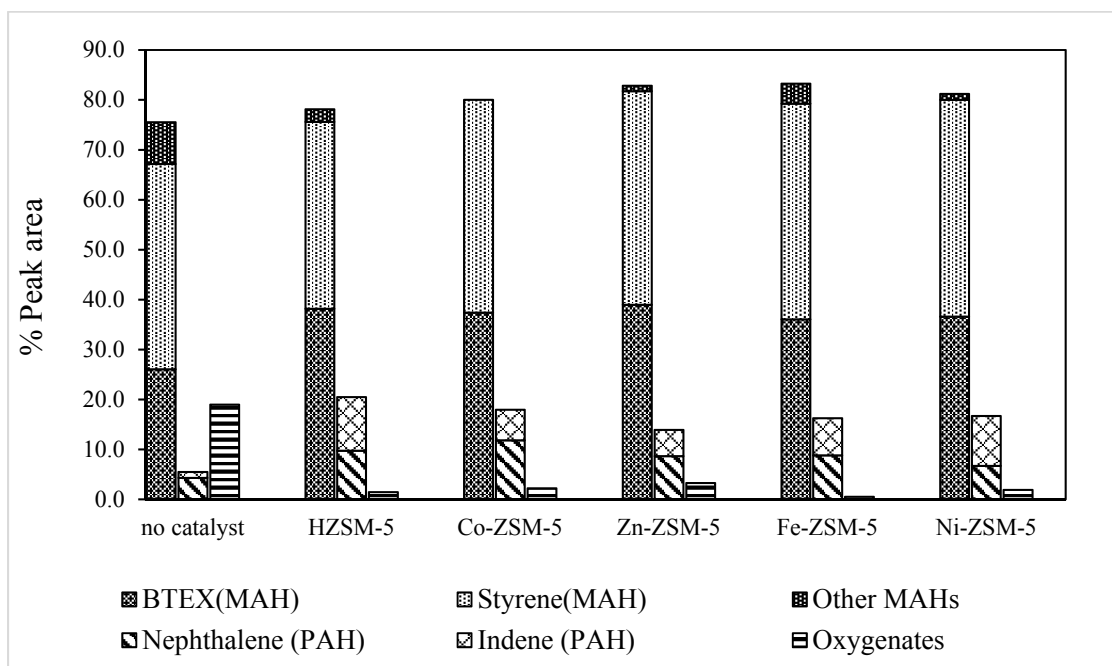


Figure 4.7: Chemical distribution of organic liquid product with and without catalyst

Addition of HZSM-5 catalyst contributed to decrease the undesired OCs noticeably, from 19% down to 1.4%, while simultaneously shifted the component distribution toward total aromatic compounds. This is attributed to the presence of highly acidic sites onto HZSM-5 which catalyzed OCs through decarbonylation, decarboxylation and dehydration followed by aromatization and cyclization reactions (Sanahuja-Parejo et al., 2018; S. Zhang et al., 2018). The reduction of OCs is an important factor for improving the quality of the liquid in terms of its heating value. As a result, production of MAHs increased/enhanced from 75.5% to 78.1%. In addition, relative yield of BTEX was increased considerably. However, highly acidic HZSM-5 also favored the formation of undesirable PAHs mainly indenenes and naphthalene, which are known as precursors to

coke formation (Fanchiang et al., 2012). Increase in relative content of PAHs is owing to the fact that in the presence of HZSM-5, biomass derived allenes could undergo alkylation with styrene, thus giving rise in indenenes formation. Also, allene could further react with indenenes resulting in naphthalene production (Zhang et al., 2016). Likewise, increase in PAHs yield over HZSM-5 was observed by (Iliopoulou et al., 2012).

On the other hand, metal substituted catalysts exhibited lesser selectivity toward PAHs generation in contrast to parent HZSM-5. This could be attributed to the anchored metal sites/ions over HZSM-5 which inhibited repolymerization reactions (Iliopoulou et al., 2014; Sun et al., 2016). More noteworthy, all four metal promoted catalysts induced a further increase in the formation of MAHs and its content reached to 82.8% in case of Zn-ZSM-5. However, MZSM-5 catalytic formulations displayed relatively high styrene yield as compared to unmodified HZSM-5. It might be speculated that metal doped HZSM-5 had mild acidic strength which led to decline in catalytic cracking. As a result, lesser conversion of styrene monomer to BTEX was observed (Botas et al., 2012). Besides, MZSM-5 showed varying degree of deoxygenation which may be ascribed to different deoxygenation mechanisms occurring within different metal loaded zeolites (Veses et al., 2015). Among all the catalysts tested, Fe-ZSM-5 exhibited the highest de-oxygenation activity.

#### **4.3.4. Physical properties of OP**

The main fuel properties of obtained pyrolytic oil in comparison with petroleum-based fuels are listed in table 4.4. The HHV of pyrolytic oil obtained by thermal pyrolysis is lower than the catalytically upgraded liquid product. It is anticipated that the decrease in oxygenated compounds during catalytic reforming turned into an increase in the heating value of upgraded liquid (Veses et al., 2015).

A slight decrease in kinematic viscosity was observed with addition of catalyst. Incorporation of all four transition metals further decreased the viscosity. However, kinematic viscosity values from thermal and catalytic co-pyrolysis were comparable to that of diesel fuel. Therefore, obtained liquid product will not likely create pumping and



atomization problems that are more common in bio-oil obtained from biomass pyrolysis alone. Moreover, the additives and preheating requirements could be avoided for catalyst upgraded co-pyrolysis oil. Besides, the density of obtained liquid products fulfill the criteria for a diesel fuel though higher than gasoline. Moreover, comparable values for non-catalytic and catalytic samples were observed for flash, fire and pour points. Flash point of obtained liquid fuel was quite low as compared to diesel, hence may lead to fire hazard and would entail additional safety measures during handling.

Table 4.4: Physical properties of liquid oil

Properties	Units	Test method	Non-catalytic	HZSM-5	MZSM-5	Diesel	Gasoline
HHV	MJ/kg	ASTM D 240	40.5	41.9	41.2 - 41.5	42-45	42-46
Density at 20 °C	g/cc	ASTM D 4052	0.89	0.89	~0.88	0.82–0.85	0.72–0.78
Kinematic Viscosity at 40 °C	cSt (mm <sup>2</sup> /s)	ASTM D244	2.96	2.53	~2.1	2–5.5	-
Flash point	°C	ASTM D 7236	~19	~19	~19	53-80	-43
Fire point	°C	ASTM D 7236	24	23.5	23	-	-
Pour Point	°C	ASTM D 97	-40	-40	-40	-40	-40 to -1

## Chapter 5 CONCLUSIONS AND RECOMMENDATIONS

### 5.1. Conclusions

In this study, co-pyrolysis of WS and PS was performed using HZSM-5 catalyst and its metal modified versions in ex-situ mode in a fixed bed reactor. The characterization of MZSM-5 catalysts confirmed the successful dispersion of metals on the surface of HZSM-5 support. However, the addition of metals resulted in the reduction of  $S_{BET}$ . Similarly,  $V_{total}$ ,  $V_{meso}$ , and  $V_{micro}$  were also found to be decreased by metal impregnation. The application of both HZSM-5 and MZSM-5 in catalytic co-pyrolysis substantially reduced the total liquid yield while simultaneously increased the formation of gaseous products in comparison to non-catalytic experimental runs. Additionally, the presence of catalysts contributed to decrease the undesired oxygenated compounds (OCs) noticeably and shifted the component distribution toward total aromatic compounds. On the other hand, incorporation of metals in HZSM-5 catalyst exhibited promising performance in lowering water content and increasing OP yield whilst reducing the coke yield by almost 50% in contrast to parent HZSM-5. MZSM-5 catalysts yielded higher styrene content in oil and exhibited lesser selectivity toward PAHs generation. Among all modified catalysts, Fe-ZSM-5 seemed to be most promising considering maximum MAHs (83.3%) and minimum OCs concentration (0.5%) in oil yield. Overall, both catalytic and non-catalytic co-pyrolytic oils showed comparable HHVs and other fuel characteristics to that of commercial fuels. However, the application of MZSM-5 produced oil with lesser OCs and PAHs, showing higher potential and lesser pre-processing requirement for use as commercial fuel.

### 5.2. Recommendations

- Efficiency of bi-metallic catalysts for upgrading must be explored
- Potential of other plastic such as HDPE and PP in metal assisted catalytic cracking should be investigated

- Use of plastic waste in comparison to virgin plastic must be studied based upon degree of pretreatment and quality of products

## REFERENCES

- Abnisa, F., & Wan Daud, W. M. A. (2014). A review on co-pyrolysis of biomass: An optional technique to obtain a high-grade pyrolysis oil. *Energy Conversion and Management*, 87, 71-85. doi:<https://doi.org/10.1016/j.enconman.2014.07.007>
- Ahmed, N., Zeeshan, M., Iqbal, N., Farooq, M. Z., & Shah, S. A. (2018). Investigation on bio-oil yield and quality with scrap tire addition in sugarcane bagasse pyrolysis. *Journal of cleaner production*, 196, 927-934.
- Aho, A., Kumar, N., Eränen, K., Salmi, T., Hupa, M., & Murzin, D. Y. J. F. (2008). Catalytic pyrolysis of woody biomass in a fluidized bed reactor: influence of the zeolite structure. 87(12), 2493-2501.
- Akhtar, J., & Saidina Amin, N. (2012). A review on operating parameters for optimum liquid oil yield in biomass pyrolysis. *Renewable and Sustainable Energy Reviews*, 16(7), 5101-5109. doi:<https://doi.org/10.1016/j.rser.2012.05.033>
- Asadullah, M., Rahman, M. A., Ali, M. M., Rahman, M. S., Motin, M. A., Sultan, M. B., & Alam, M. R. (2007). Production of bio-oil from fixed bed pyrolysis of bagasse. *Fuel*, 86(16), 2514-2520. doi:<https://doi.org/10.1016/j.fuel.2007.02.007>
- Ateş, F., Pütün, E., Pütün, A. J. o. A., & Pyrolysis, A. (2004). Fast pyrolysis of sesame stalk: yields and structural analysis of bio-oil. 71(2), 779-790.
- Balasundram, V., Zaman, K. K., Ibrahim, N., Kasmani, R. M., Isha, R., Hamid, M. K. A., & Hasbullah, H. J. J. o. A. (2018). Catalytic upgrading of pyrolysis vapours over metal modified HZSM-5 via in-situ pyrolysis of sugarcane bagasse: Effect of nickel to cerium ratio on HZSM-5. *Journal of Analytical and Applied Pyrolysis*.
- Botas, J. A., Serrano, D. P., García, A., de Vicente, J., & Ramos, R. (2012). Catalytic conversion of rapeseed oil into raw chemicals and fuels over Ni- and Mo-modified nanocrystalline ZSM-5 zeolite. *Catalysis Today*, 195(1), 59-70. doi:<https://doi.org/10.1016/j.cattod.2012.04.061>
- Brebu, M., Ucar, S., Vasile, C., & Yanik, J. (2010). Co-pyrolysis of pine cone with synthetic polymers. *Fuel*, 89(8), 1911-1918.
- Bridgwater, A. V. J. B., & bioenergy. (2012). Review of fast pyrolysis of biomass and product upgrading. 38, 68-94.
- Bulushev, D. A., & Ross, J. R. H. (2011). Catalysis for conversion of biomass to fuels via pyrolysis and gasification: A review. *Catalysis Today*, 171(1), 1-13. doi:<https://doi.org/10.1016/j.cattod.2011.02.005>
- Carpenter, D., Westover, T. L., Czernik, S., & Jablonski, W. (2014). Biomass feedstocks for renewable fuel production: a review of the impacts of feedstock and pretreatment on the yield and product distribution of fast pyrolysis bio-oils and vapors. *Green Chemistry*, 16(2), 384-406. doi:10.1039/C3GC41631C
- Collard, F.-X., & Blin, J. (2014). A review on pyrolysis of biomass constituents: Mechanisms and composition of the products obtained from the conversion of cellulose, hemicelluloses and lignin. *Renewable and Sustainable Energy Reviews*, 38, 594-608. doi:<https://doi.org/10.1016/j.rser.2014.06.013>
- Dewangan, A., Pradhan, D., & Singh, R. K. (2016). Co-pyrolysis of sugarcane bagasse and low-density polyethylene: Influence of plastic on pyrolysis product yield. *Fuel*, 185, 508-516. doi:<https://doi.org/10.1016/j.fuel.2016.08.011>
- Dickerson, T., & Soria, J. (2013). *Catalytic Fast Pyrolysis: A Review* (Vol. 6).
- Dorado, C., Mullen, C. A., & Boateng, A. A. (2015). Origin of carbon in aromatic and olefin products derived from HZSM-5 catalyzed co-pyrolysis of cellulose and plastics via isotopic labeling. *Applied Catalysis B: Environmental*, 162, 338-345. doi:<https://doi.org/10.1016/j.apcatb.2014.07.006>

- Duan, D., Wang, Y., Dai, L., Ruan, R., Zhao, Y., Fan, L., . . . Liu, Y. (2017). Ex-situ catalytic co-pyrolysis of lignin and polypropylene to upgrade bio-oil quality by microwave heating. *Bioresource Technology*, *241*, 207-213.
- Dutta, A., Sahir, A., Tan, E., Humbird, D., Snowden-Swan, L. J., Meyer, P. A., . . . Lukas, J. (2015). *Process design and economics for the conversion of lignocellulosic biomass to hydrocarbon fuels: Thermochemical research pathways with in situ and ex situ upgrading of fast pyrolysis vapors*. Retrieved from
- Elsayed, I., & Eseyin, A. (2016). Production high yields of aromatic hydrocarbons through catalytic fast pyrolysis of torrefied wood and polystyrene. *Fuel*, *174*, 317-324.
- Fanchiang, W.-L., & Lin, Y.-C. J. A. C. A. G. (2012). Catalytic fast pyrolysis of furfural over H-ZSM-5 and Zn/H-ZSM-5 catalysts. *Applied Catalysis A: General*, *419*, 102-110.
- Farooq, M. Z., Zeeshan, M., Iqbal, S., Ahmed, N., & Shah, S. A. Y. (2018a). Influence of waste tire addition on wheat straw pyrolysis yield and oil quality. *Energy*, *144*, 200-206.
- Farooq, M. Z., Zeeshan, M., Iqbal, S., Ahmed, N., & Shah, S. A. Y. J. E. (2018b). Influence of waste tire addition on wheat straw pyrolysis yield and oil quality. *144*, 200-206.
- French, R., & Czernik, S. (2010). Catalytic pyrolysis of biomass for biofuels production. *Fuel Processing Technology*, *91*(1), 25-32. doi:<https://doi.org/10.1016/j.fuproc.2009.08.011>
- Fu, P., Bai, X., Yi, W., Li, Z., Li, Y. J. E. C., & Management. (2018). Fast pyrolysis of wheat straw in a dual concentric rotary cylinder reactor with ceramic balls as recirculated heat carrier. *171*, 855-862.
- Ghorbannezhad, P., Firouzabadi, M. D., Ghasemian, A., de Wild, P. J., Heeres, H. J. J. o. A., & Pyrolysis, A. (2018). Sugarcane bagasse ex-situ catalytic fast pyrolysis for the production of Benzene, Toluene and Xylenes (BTX). *Journal of Analytical and Applied Pyrolysis*, *131*, 1-8.
- Gollakota, A. R. K., Reddy, M., Subramanyam, M. D., & Kishore, N. (2016). A review on the upgradation techniques of pyrolysis oil. *Renewable and Sustainable Energy Reviews*, *58*, 1543-1568. doi:<https://doi.org/10.1016/j.rser.2015.12.180>
- Guda, V. K., & Toghiani, H. (2016). Altering bio-oil composition by catalytic treatment of pinewood pyrolysis vapors over zeolites using an auger - packed bed integrated reactor system %J *Biofuel Research Journal*, *3*(3), 448-457. doi:10.18331/brj2016.3.3.4
- Güngör, A., Önenç, S., Uçar, S., & Yanik, J. (2012). Comparison between the “one-step” and “two-step” catalytic pyrolysis of pine bark. *Journal of Analytical and Applied Pyrolysis*, *97*, 39-48. doi:<https://doi.org/10.1016/j.jaap.2012.06.011>
- Hassan, E. B., Elsayed, I., & Eseyin, A. (2016). Production high yields of aromatic hydrocarbons through catalytic fast pyrolysis of torrefied wood and polystyrene. *Fuel*, *174*, 317-324. doi:<https://doi.org/10.1016/j.fuel.2016.02.031>
- Hassan, H., Lim, J. K., & Hameed, B. H. (2016). Recent progress on biomass co-pyrolysis conversion into high-quality bio-oil. *Bioresource Technology*, *221*, 645-655. doi:<https://doi.org/10.1016/j.biortech.2016.09.026>
- Hu, C., Xiao, R., & Zhang, H. (2017). Ex-situ catalytic fast pyrolysis of biomass over HZSM-5 in a two-stage fluidized-bed/fixed-bed combination reactor. *Bioresource Technology*, *243*, 1133-1140.
- Huang, W., Gong, F., Fan, M., Zhai, Q., Hong, C., & Li, Q. J. B. t. (2012). Production of light olefins by catalytic conversion of lignocellulosic biomass with HZSM-5 zeolite impregnated with 6 wt.% lanthanum. *121*, 248-255.
- Huang, Y., Wei, L., Julson, J., Gao, Y., & Zhao, X. (2015). Converting pine sawdust to advanced biofuel over HZSM-5 using a two-stage catalytic pyrolysis reactor. *Journal of Analytical and Applied Pyrolysis*, *111*, 148-155. doi:<https://doi.org/10.1016/j.jaap.2014.11.019>
- Iisa, K., French, R. J., Orton, K. A., Yung, M. M., Johnson, D. K., ten Dam, J., . . . Nimlos, M. R. (2016). In situ and ex situ catalytic pyrolysis of pine in a bench-scale fluidized bed reactor system. *Energy & Fuels*, *30*(3), 2144-2157.
- Iliopoulou, E., Stefanidis, S., Kalogiannis, K., Psarras, A., Delimitis, A., Triantafyllidis, K., & Lappas, A. (2014). Pilot-scale validation of Co-ZSM-5 catalyst performance in the catalytic upgrading of biomass pyrolysis vapours. *Green Chemistry*, *16*(2), 662-674.
- Iliopoulou, E. F., Stefanidis, S. D., Kalogiannis, K. G., Delimitis, A., Lappas, A. A., & Triantafyllidis, K. S. (2012). Catalytic upgrading of biomass pyrolysis vapors using transition metal-modified

- ZSM-5 zeolite. *Applied Catalysis B: Environmental*, 127, 281-290. doi:<https://doi.org/10.1016/j.apcatb.2012.08.030>
- Islam, M., Ali, M. H., & Haziq, M. (2017). *Fixed bed pyrolysis of biomass solid waste for bio-oil* (Vol. 1875).
- Jahirul, M. I., Rasul, M. G., Chowdhury, A. A., & Ashwath, N. (2012). Biofuels production through biomass pyrolysis—a technological review. *Energies*, 5(12), 4952-5001.
- Kabir, G., & Hameed, B. (2017). Recent progress on catalytic pyrolysis of lignocellulosic biomass to high-grade bio-oil and bio-chemicals. *Renewable and Sustainable Energy Reviews*, 70, 945-967.
- Kantarelis, E., Yang, W., & Blasiak, W. (2014). Effect of zeolite to binder ratio on product yields and composition during catalytic steam pyrolysis of biomass over transition metal modified HZSM5. *Fuel*, 122, 119-125. doi:<https://doi.org/10.1016/j.fuel.2013.12.054>
- Kim, B.-S., Kim, Y.-M., Jae, J., Watanabe, C., Kim, S., Jung, S.-C., . . . Park, Y.-K. (2015). Pyrolysis and catalytic upgrading of Citrus unshiu peel. *Bioresource Technology*, 194, 312-319. doi:<https://doi.org/10.1016/j.biortech.2015.07.035>
- Kim, Y.-M., Jae, J., Kim, B.-S., Hong, Y., Jung, S.-C., & Park, Y.-K. (2017). Catalytic co-pyrolysis of torrefied yellow poplar and high-density polyethylene using microporous HZSM-5 and mesoporous Al-MCM-41 catalysts. *Energy Conversion and Management*, 149, 966-973.
- Kumar, G., Panda, A. K., & Singh, R. K. (2010). Optimization of process for the production of bio-oil from eucalyptus wood. *Journal of Fuel Chemistry and Technology*, 38(2), 162-167. doi:[https://doi.org/10.1016/S1872-5813\(10\)60028-X](https://doi.org/10.1016/S1872-5813(10)60028-X)
- Lappas, A. A., Kalogiannis, K. G., Iliopoulou, E. F., Triantafyllidis, K. S., Stefanidis, S. D. J. W. I. R. E., & Environment. (2012). Catalytic pyrolysis of biomass for transportation fuels. 1(3), 285-297.
- Lazaridis, P. A., Fotopoulos, A. P., Karakoulia, S. A., & Triantafyllidis, K. S. J. F. i. c. (2018). Catalytic fast pyrolysis of kraft lignin with conventional, mesoporous and nanosized ZSM-5 zeolite for the production of alkyl-phenols and aromatics. 6.
- Li, P., Li, D., Yang, H., Wang, X., & Chen, H. (2016). Effects of Fe-, Zr-, and Co-Modified Zeolites and Pretreatments on Catalytic Upgrading of Biomass Fast Pyrolysis Vapors. *Energy & Fuels*, 30(4), 3004-3013. doi:10.1021/acs.energyfuels.5b02894
- Li, X., Li, J., Zhou, G., Feng, Y., Wang, Y., Yu, G., . . . Wang, B. (2014). Enhancing the production of renewable petrochemicals by co-feeding of biomass with plastics in catalytic fast pyrolysis with ZSM-5 zeolites. *Applied Catalysis A: General*, 481, 173-182. doi:<https://doi.org/10.1016/j.apcata.2014.05.015>
- Li, X., Zhang, H., Li, J., Su, L., Zuo, J., Komarneni, S., & Wang, Y. (2013). Improving the aromatic production in catalytic fast pyrolysis of cellulose by co-feeding low-density polyethylene. *Applied Catalysis A: General*, 455, 114-121. doi:<https://doi.org/10.1016/j.apcata.2013.01.038>
- Lin, X., Zhang, Z., Tan, S., Wang, F., Song, Y., Wang, Q., & Pittman Jr, C. U. (2017). In line wood plastic composite pyrolyses and HZSM-5 conversion of the pyrolysis vapors. *Energy Conversion and Management*, 141, 206-215.
- Liu, S., Zhang, Y., Fan, L., Zhou, N., Tian, G., Zhu, X., . . . Ruan, R. (2017). Bio-oil production from sequential two-step catalytic fast microwave-assisted biomass pyrolysis. *Fuel*, 196, 261-268. doi:<https://doi.org/10.1016/j.fuel.2017.01.116>
- Liu, T.-L., Cao, J.-P., Zhao, X.-Y., Wang, J.-X., Ren, X.-Y., Fan, X., . . . Wei, X.-Y. (2017). In situ upgrading of Shengli lignite pyrolysis vapors over metal-loaded HZSM-5 catalyst. *Fuel Processing Technology*, 160, 19-26.
- Lu, Q., Zhang, Z.-b., Ye, X.-n., Li, W.-t., Hu, B., Dong, C.-q., & Yang, Y.-p. (2017). Selective production of 4-ethyl guaiacol from catalytic fast pyrolysis of softwood biomass using Pd/SBA-15 catalyst. *Journal of Analytical and Applied Pyrolysis*, 123, 237-243.
- Mantilla, S. V., Gauthier-Maradei, P., Gil, P. A., Cárdenas, S. T. J. J. o. A., & Pyrolysis, A. (2014). Comparative study of bio-oil production from sugarcane bagasse and palm empty fruit bunch: yield optimization and bio-oil characterization. 108, 284-294.
- Mendes, F. L., Ximenes, V. L., de Almeida, M. B. B., Azevedo, D. A., Tessarolo, N. S., & de Rezende Pinho, A. (2016). Catalytic pyrolysis of sugarcane bagasse and pinewood in a pilot scale unit. *Journal of Analytical and Applied Pyrolysis*, 122, 395-404. doi:<https://doi.org/10.1016/j.jaap.2016.08.001>

- Miao, X., Wu, Q., Yang, C. J. J. o. a., & pyrolysis, a. (2004). Fast pyrolysis of microalgae to produce renewable fuels. *71*(2), 855-863.
- Mihalcik, D. J., Mullen, C. A., & Boateng, A. A. (2011). Screening acidic zeolites for catalytic fast pyrolysis of biomass and its components. *Journal of Analytical and Applied Pyrolysis*, *92*(1), 224-232. doi:https://doi.org/10.1016/j.jaap.2011.06.001
- Mirza, U. K., Ahmad, N., & Majeed, T. (2008). An overview of biomass energy utilization in Pakistan. *Renewable and Sustainable Energy Reviews*, *12*(7), 1988-1996.
- Mohammed, I., Kazi, F., Suzana, Y., Alaba, P., Sani, Y. M., & Abakr, Y. A. (2016). *Catalytic Intermediate Pyrolysis of Napier Grass in a Fixed Bed Reactor with ZSM-5, HZSM-5 and Zinc-Exchanged Zeolite-A as the Catalyst*.
- Mohan, D., Pittman, C. U., & Steele, P. H. (2006). Pyrolysis of Wood/Biomass for Bio-oil: A Critical Review. *Energy & Fuels*, *20*(3), 848-889. doi:10.1021/ef0502397
- Muley, P. D., Henkel, C., Abdollahi, K. K., & Boldor, D. (2015). Pyrolysis and catalytic upgrading of pinewood sawdust using an induction heating reactor. *Energy & Fuels*, *29*(11), 7375-7385.
- Mullen, C. A., Dorado, C., & Boateng, A. A. (2017). Catalytic co-pyrolysis of switchgrass and polyethylene over HZSM-5: Catalyst deactivation and coke formation. *Journal of Analytical and Applied Pyrolysis*.
- Naqvi, S. R., Jamshaid, S., Naqvi, M., Farooq, W., Niazi, M. B. K., Aman, Z., . . . Afzal, W. (2018). Potential of biomass for bioenergy in Pakistan based on present case and future perspectives. *Renewable and Sustainable Energy Reviews*, *81*, 1247-1258. doi:https://doi.org/10.1016/j.rser.2017.08.012
- Onay, Ö., Beis, S., Koçkar, Ö. M. J. J. o. a., & pyrolysis, a. (2001). Fast pyrolysis of rape seed in a well-swept fixed-bed reactor. *58*, 995-1007.
- Pütün, A., Koçkar, Ö., Yorgun, S., Gerçel, H., Andresen, J., Snape, C., & Pütün, E. J. F. P. T. (1996). Fixed-bed pyrolysis and hydrolysis of sunflower bagasse: product yields and compositions. *46*(1), 49-62.
- Pütün, A. E., Apaydın, E., & Pütün, E. J. E. (2004). Rice straw as a bio-oil source via pyrolysis and steam pyrolysis. *29*(12-15), 2171-2180.
- Pütün, A. E., Gerçel, H. F., Koçkar, Ö. M., Ege, Ö., Snape, C. E., & Pütün, E. J. F. (1996). Oil production from an arid-land plant: fixed-bed pyrolysis and hydrolysis of *Euphorbia rigida*. *75*(11), 1307-1312.
- Pütün, E., Uzun, B. B., Pütün, A. e. E. J. E., & Fuels. (2009). Rapid pyrolysis of olive residue. 2. Effect of catalytic upgrading of pyrolysis vapors in a two-stage fixed-bed reactor. *23*(4), 2248-2258.
- Rafique, M. M., & Rehman, S. (2017). National energy scenario of Pakistan—Current status, future alternatives, and institutional infrastructure: An overview. *Renewable and Sustainable Energy Reviews*, *69*, 156-167.
- Rafique, M. M., & Rehman, S. (2017). National energy scenario of Pakistan – Current status, future alternatives, and institutional infrastructure: An overview. *Renewable and Sustainable Energy Reviews*, *69*, 156-167. doi:https://doi.org/10.1016/j.rser.2016.11.057
- Rahman, M. M., Liu, R., & Cai, J. (2018). Catalytic fast pyrolysis of biomass over zeolites for high quality bio-oil – A review. *Fuel Processing Technology*, *180*, 32-46. doi:https://doi.org/10.1016/j.fuproc.2018.08.002
- Ren, X.-Y., Cao, J.-P., Zhao, X.-Y., Shen, W.-Z., Wei, X.-Y. J. J. o. A., & Pyrolysis, A. (2018). Increasing light aromatic products during upgrading of lignite pyrolysis vapor over Co-modified HZSM-5. *Journal of Analytical and Applied Pyrolysis*, *130*, 190-197.
- Rezaei, P. S., Oh, D., Hong, Y., Kim, Y.-M., Jae, J., Jung, S.-C., . . . Park, Y.-K. (2017). In-situ catalytic co-pyrolysis of yellow poplar and high-density polyethylene over mesoporous catalysts. *Energy Conversion and Management*, *151*, 116-122.
- Ro, D., Kim, Y.-M., Lee, I.-G., Jae, J., Jung, S.-C., Kim, S. C., & Park, Y.-K. J. J. o. C. P. (2018). Bench scale catalytic fast pyrolysis of empty fruit bunches over low cost catalysts and HZSM-5 using a fixed bed reactor. *Journal of Cleaner Production*, *176*, 298-303.
- Sanahuja-Parejo, O., Veses, A., Navarro, M., López, J., Murillo, R., Callén, M., & García, T. J. C. E. J. (2018). Drop-in biofuels from the co-pyrolysis of grape seeds and polystyrene. *Chemical Engineering Journal*.

- Saraçoğlu, E., Uzun, B. B., & Apaydın-Varol, E. (2017). Upgrading of fast pyrolysis bio-oil over Fe modified ZSM-5 catalyst to enhance the formation of phenolic compounds. *International Journal of Hydrogen Energy*, *42*(33), 21476-21486.
- Sebestyén, Z., Barta-Rajnai, E., Bozi, J., Blazsó, M., Jakab, E., Miskolczi, N., . . . Czégény, Z. (2017). Thermo-catalytic pyrolysis of biomass and plastic mixtures using HZSM-5. *Applied Energy*, *207*, 114-122.
- Şensöz, S., Demiral, İ., & Gerçel, H. F. J. B. t. (2006). Olive bagasse (*Olea europea* L.) pyrolysis. *97*(3), 429-436.
- Shah, S. A. Y., Zeeshan, M., Farooq, M. Z., Ahmed, N., & Iqbal, N. (2019). Co-pyrolysis of cotton stalk and waste tire with a focus on liquid yield quantity and quality. *Renewable Energy*, *130*, 238-244. doi:<https://doi.org/10.1016/j.renene.2018.06.045>
- Smets, K., Roukaerts, A., Czech, J., Reggers, G., Schreurs, S., Carleer, R., & Yperman, J. (2013). Slow catalytic pyrolysis of rapeseed cake: Product yield and characterization of the pyrolysis liquid. *Biomass and Bioenergy*, *57*, 180-190. doi:<https://doi.org/10.1016/j.biombioe.2013.07.001>
- Stefanidis, S., Kalogiannis, K., Iliopoulou, E., Lappas, A., & Pilavachi, P. J. B. t. (2011). In-situ upgrading of biomass pyrolysis vapors: catalyst screening on a fixed bed reactor. *102*(17), 8261-8267.
- Sun, L., Zhang, X., Chen, L., Zhao, B., Yang, S., & Xie, X. (2016). Comparison of catalytic fast pyrolysis of biomass to aromatic hydrocarbons over ZSM-5 and Fe/ZSM-5 catalysts. *Journal of Analytical and Applied Pyrolysis*, *121*, 342-346. doi:<https://doi.org/10.1016/j.jaap.2016.08.015>
- Uzoejinwa, B. B., He, X., Wang, S., Abomohra, A. E.-F., Hu, Y., Wang, Q. J. E. C., & Management. (2018). Co-pyrolysis of biomass and waste plastics as a thermochemical conversion technology for high-grade biofuel production: Recent progress and future directions elsewhere worldwide. *163*, 468-492.
- Uzun, B. B., & Sarioğlu, N. J. F. P. T. (2009). Rapid and catalytic pyrolysis of corn stalks. *90*(5), 705-716.
- Valle, B., Gayubo, A. G., Aguayo, A. T., Olazar, M., Bilbao, J. J. E., & Fuels. (2010). Selective production of aromatics by crude bio-oil valorization with a nickel-modified HZSM-5 zeolite catalyst. *Energy*, *24*(3), 2060-2070.
- Veses, A., Puértolas, B., Callén, M. S., & García, T. (2015). Catalytic upgrading of biomass derived pyrolysis vapors over metal-loaded ZSM-5 zeolites: Effect of different metal cations on the bio-oil final properties. *Microporous and Mesoporous Materials*, *209*, 189-196. doi:<https://doi.org/10.1016/j.micromeso.2015.01.012>
- Vichaphund, S., Aht-ong, D., Sricharoenchaikul, V., & Atong, D. (2015). Production of aromatic compounds from catalytic fast pyrolysis of *Jatropha* residues using metal/HZSM-5 prepared by ion-exchange and impregnation methods. *Renewable Energy*, *79*, 28-37. doi:<https://doi.org/10.1016/j.renene.2014.10.013>
- Wang, K., Zheng, Y., Zhu, X., Brewer, C. E., & Brown, R. C. (2017). Ex-situ catalytic pyrolysis of wastewater sewage sludge—A micro-pyrolysis study. *Bioresource Technology*, *232*, 229-234.
- Wang, L., Lei, H., Bu, Q., Ren, S., Wei, Y., Zhu, L., . . . Tang, J. (2014). Aromatic hydrocarbons production from ex situ catalysis of pyrolysis vapor over Zinc modified ZSM-5 in a packed-bed catalysis coupled with microwave pyrolysis reactor. *Fuel*, *129*, 78-85. doi:<https://doi.org/10.1016/j.fuel.2014.03.052>
- Wang, L., Lei, H., Lee, J., Chen, S., Tang, J., & Ahiring, B. (2013). Aromatic hydrocarbons production from packed-bed catalysis coupled with microwave pyrolysis of Douglas fir sawdust pellets. *RSC Advances*, *3*(34), 14609-14615.
- Wang, Y., Dai, L., Fan, L., Cao, L., Zhou, Y., Zhao, Y., . . . Ruan, R. (2017). Catalytic co-pyrolysis of waste vegetable oil and high density polyethylene for hydrocarbon fuel production. *Waste Management*, *61*, 276-282.
- Wang, Y., & Wang, J. (2016). Multifaceted effects of HZSM-5 (Proton-exchanged Zeolite Socony Mobil-5) on catalytic cracking of pinewood pyrolysis vapor in a two-stage fixed bed reactor. *Bioresource Technology*, *214*, 700-710. doi:<https://doi.org/10.1016/j.biortech.2016.05.027>
- Xue, Y., Kelkar, A., & Bai, X. (2016). Catalytic co-pyrolysis of biomass and polyethylene in a tandem micro-pyrolyzer. *Fuel*, *166*, 227-236.



- Yaman, E., Yargic, A. S., Ozbay, N., Uzun, B. B., Kalogiannis, K. G., Stefanidis, S. D., . . . Lappas, A. A. J. J. o. C. P. (2018). Catalytic upgrading of pyrolysis vapours: Effect of catalyst support and metal type on phenolic content of bio-oil. *Journal of cleaner production*, *185*, 52-61.
- Yildiz, G., Ronsse, F., Duren, R. v., & Prins, W. (2016). Challenges in the design and operation of processes for catalytic fast pyrolysis of woody biomass. *Renewable and Sustainable Energy Reviews*, *57*, 1596-1610. doi:<https://doi.org/10.1016/j.rser.2015.12.202>
- Zhang, B., Zhong, Z., Ding, K., & Song, Z. (2015). Production of aromatic hydrocarbons from catalytic co-pyrolysis of biomass and high density polyethylene: Analytical Py–GC/MS study. *Fuel*, *139*, 622-628. doi:<https://doi.org/10.1016/j.fuel.2014.09.052>
- Zhang, H., Likun, P. K. W., & Xiao, R. J. S. o. T. T. E. (2018). Improving the hydrocarbon production via co-pyrolysis of bagasse with bio-plastic and dual-catalysts layout. *618*, 151-156.
- Zhang, H., Nie, J., Xiao, R., Jin, B., Dong, C., & Xiao, G. (2014). Catalytic co-pyrolysis of biomass and different plastics (polyethylene, polypropylene, and polystyrene) to improve hydrocarbon yield in a fluidized-bed reactor. *Energy & Fuels*, *28*(3), 1940-1947.
- Zhang, S., Zhang, H., Liu, X., Zhu, S., Hu, L., & Zhang, Q. J. F. P. T. (2018). Upgrading of bio-oil from catalytic pyrolysis of pretreated rice husk over Fe-modified ZSM-5 zeolite catalyst. *Fuel Processing Technology*, *175*, 17-25.
- Zhang, X., Lei, H., Chen, S., & Wu, J. (2016). Catalytic co-pyrolysis of lignocellulosic biomass with polymers: a critical review. *Green Chemistry*, *18*(15), 4145-4169.
- Zheng, Y., Wang, F., Yang, X., Huang, Y., Liu, C., Zheng, Z., & Gu, J. (2017). Study on aromatics production via the catalytic pyrolysis vapor upgrading of biomass using metal-loaded modified H-ZSM-5. *Journal of Analytical and Applied Pyrolysis*, *126*, 169-179.